Cellular/Molecular

Hydrogen Peroxide Gates a Voltage-Dependent Cation Current in *Aplysia* Neuroendocrine Cells

Alamjeet K. Chauhan and Neil S. Magoski

Department of Biomedical and Molecular Sciences, Experimental Medicine Graduate Program and Centre for Neuroscience Studies, Queen's University, Kingston, Ontario K7L 3N6, Canada

Nonselective cation channels promote persistent spiking in many neurons from a diversity of animals. In the hermaphroditic marine-snail, *Aplysia californica*, synaptic input to the neuroendocrine bag cell neurons triggers various cation channels, causing an ~30 min afterdischarge of action potentials and the secretion of egg-laying hormone. During the afterdischarge, protein kinase C is also activated, which in turn elevates hydrogen peroxide (H_2O_2), likely by stimulating nicotinamide adenine dinucleotide phosphate oxidase. The present study investigated whether H_2O_2 regulates cation channels to drive the afterdischarge. In single, cultured bag cell neurons, H_2O_2 elicited a prolonged, concentration- and voltage-dependent inward current, associated with an increase in membrane conductance and a reversal potential of ~+30 mV. Compared with normal saline, the presence of Ca^{2+}-free, Na^+-free, or Na^+/Ca^{2+}-free extracellular saline, lowered the current amplitude and left-shifted the reversal potential, consistent with a nonselective cationic conductance. Preventing H_2O_2 reduction with the glutathione peroxidase inhibitor, mercaptosuccinate, enhanced the H_2O_2-induced current, while boosting glutathione production with its precursor, *N*-acetylcysteine, or adding the reducing agent, dithiothreitol, lessened the response. Moreover, the current generated by the alkylating agent, *N*-ethylmaleimide, occluded the effect of H_2O_2. The H_2O_2-induced current was inhibited by tetrodotoxin as well as the cation channel blockers, 9-phenanthrol and clotrimazole. In current-clamp, H_2O_2 stimulated burst firing, but this was attenuated or prevented altogether by the channel blockers. Finally, H_2O_2 evoked an afterdischarge from whole bag cell neuron clusters recorded *ex vivo* by sharp-electrode. H_2O_2 may regulate a cation channel to influence long-term changes in activity and ultimately reproduction.

Key words: **bursting; H_2O_2; mollusk; peptidergic neuron; redox; reproduction**

Significance Statement

Hydrogen peroxide (H_2O_2) is often studied in a pathological context, such as ischemia or inflammation. However, H_2O_2 also physiologically modulates synaptic transmission and gates certain transient receptor potential channels. That stated, the effect of H_2O_2 on neuronal excitability remains less well defined. Here, we examine how H_2O_2 influences *Aplysia* bag cell neurons, which elicit ovulation by releasing hormones during an afterdischarge. These neuroendocrine cells are uniquely identifiable and amenable to recording as individual cultured neurons or a cluster from the nervous system. In both culture and the cluster, H_2O_2 evokes prolonged, afterdischarge-like bursting by gating a nonselective voltage-dependent cationic current. Thus, H_2O_2, which is generated in response to afterdischarge-associated second messengers, may prompt the firing necessary for hormone secretion and procreation.

Introduction

Reactive oxygen species are generated either as a byproduct of oxidative metabolism (Babior et al., 1973; Kourie, 1998) or via NADPH oxidase (Bedard and Krause, 2007). O_2 is reduced to the superoxide anion radical, $O_2^{\cdot-}$, which is in turn dismutated to the more stable and freely diffusible hydrogen peroxide (H_2O_2; Brookes et al., 2004; Bedard and Krause, 2007; Lee et al., 2015a). Elevated reactive oxygen species can lead to stress and cell death, potentially contributing to aging (Sohal and Orr, 2012) or Alzheimer's and Parkinson's diseases (Hernandes and Britto, 2012). However, growing evidence shows that H_2O_2 may regulate ion

Received March 28, 2019; revised Oct. 7, 2019; accepted Oct. 27, 2019.

Author contributions: A.K.C. and N.S.M. designed research; A.K.C. performed research; A.K.C. and N.S.M. analyzed data; A.K.C. and N.S.M. wrote the paper.

This work was supported by a Canadian Institutes of Health Research operating Grant (MOP111211) and project Grant (PJT-159794) to N.S.M. We thank C. A. London for technical support, and C. B. Beekharry and C. J. Groten for preliminary assistance with the H_2O_2-induced response.

The authors declare no competing financial interests.

Correspondence should be addressed to Neil S. Magoski at magoski@queensu.ca.

https://doi.org/10.1523/JNEUROSCI.1460-19.2019

channels physiologically; for example, in the substantia nigra, H_2O_2 hyperpolarizes dopaminergic neurons by gating an ATP-sensitive K^+ channel, and depolarizes GABAergic neurons by gating a nonselective cation channel (Avshalumov et al., 2005; Lee et al., 2011).

Cation channels underlie bursting and persistent firing in many neurons (Partridge et al., 1994; Major and Tank, 2004). This includes cation channel-dependent protracted spiking in the snails, *Aplysia* (Kramer and Zucker, 1985; Matsumoto et al., 1988), *Archidoris* (Partridge et al., 1979), and *Helix* (Swandulla and Lux, 1985; Partridge and Swandulla, 1987). For rodents, cation channels mediate long-lasting activity in lumbosacral spinal cord (Derjean et al., 2005), dorsal horn (Morisset and Nagy, 2000), olfactory bulb (Shpak et al., 2012), substantia nigra (Mrejeru et al., 2011), and rostral ambiguus (Rekling and Feldman, 1997), as well as hippocampal (Knauer et al., 2013), anterior cingulate (Ratté et al., 2018), entorhinal (Tahvildari et al., 2008), and prefrontal cortex (Yan et al., 2009; Baker et al., 2018). Functionally, cation channels impact memory (Egorov et al., 2002; Sidiropoulou et al., 2009), sensory coding (Dong et al., 2009), motor pattern generation (Di Prisco et al., 1997), and neuroendocrine control (Chakfe and Bourque, 2000).

The bag cell neurons are neuroendocrine cells that initiate reproduction in *Aplysia* (Conn and Kaczmarek, 1989; Zhang and Kaczmarek, 2008; Sturgeon et al., 2018). In response to cholinergic input, these neurons depolarize and undergo a lengthy afterdischarge, with both a fast-phase (~5 Hz, ~1 min) and slow-phase (1 Hz, ~30 min) of action potential firing that results in the neurohemal secretion of egg-laying hormone (Kupfermann and Kandel, 1970; Arch, 1972; Pinsker and Dudek, 1977; Loechner et al., 1990; Roubos et al., 1990; Michel and Wayne, 2002; Hatcher and Sweedler, 2008; White and Magoski, 2012). The hormone engages both central neurons and peripheral organs to induce behaviors that culminate in the deposition of fertilized eggs (Arch and Smock, 1977; Stuart and Strumwasser, 1980; Rothman et al., 1983). The afterdischarge is maintained by opening of three, distinct cation channels: a voltage-independent channel gated by calmodulin-kinase (Hung and Magoski, 2007; Hickey et al., 2010), a separate voltage-independent channel triggered by diacylglycerol (DAG; Sturgeon and Magoski, 2016), and a Ca^{2+}-permeable, Ca^{2+}-activated, voltage-dependent channel (Wilson et al., 1996; Lupinsky and Magoski, 2006; Geiger et al., 2009). Munnamalai et al. (2014) showed that NADPH oxidase is present in bag cell neurons, and protein kinase C (PKC), which is activated early in the slow-phase of the afterdischarge (Wayne et al., 1999), stimulates H_2O_2 production. This likely occurs through PKC-mediated phosphorylation of the NADPH oxidase cytosolic regulatory subunit, $p47^{phox}$ (Fontayne et al., 2002). Thus, we sought to test whether H_2O_2 can affect bag cell neuron function in a manner concordant with afterdischarge generation. The present study shows that exogenous H_2O_2 triggers a conductance similar to the voltage-dependent cation channel previously characterized in bag cell neurons. This H_2O_2-induced current is sensitive to both changes in redox and cation channel blockers; moreover, it produces prolonged depolarization and firing. Historically, excessive H_2O_2 has been implicated in neuronal cell death (Herson and Ashford, 1997; Herson et al., 1999; Smith et al., 2003); however, along with work on substantia nigra (Lee et al., 2011, 2013) and hippocampal (Olah et al., 2009) neurons, our results suggest a role for H_2O_2 in regulating persistent firing. In *Aplysia*, such regulation may have consequences for procreation.

Materials and Methods

Animals and cell culture. Adult *Aplysia californica* (a hermaphrodite) weighing 200–650 g were obtained from Marinus and housed in an ~300 L aquarium containing continuously circulating, aerated sea water (Instant Ocean, Aquarium Systems) at 16–18°C on a 12:12 h light/dark cycle and fed romaine lettuce five times/week. All experiments were approved by the Queen's University Animal Care Committee (protocols 2013-041 and 2017-1745).

For primary cultures of isolated bag cell neurons, animals were anesthetized by an injection of isotonic $MgCl_2$ (0.39 M; volume ~50% of body weight), and the abdominal ganglion was removed and treated with dispase II (13.3 mg/ml; 04942078601, Roche Diagnostics/Sigma-Aldrich) dissolved in tissue culture artificial sea water (tcASW; composition in mM: 460 NaCl, 10.4 KCl, 11 $CaCl_2$, 55 $MgCl_2$, 15 HEPES, 1 mg/ml glucose, 100 U/ml penicillin plus 0.1 mg/ml streptomycin (P4333, Sigma-Aldrich), pH 7.8 with NaOH, for 18 h at 22°C. The ganglion was then rinsed in tcASW for 1 h, and the two bag cell neuron clusters were dissected from their surrounding connective tissue. Using a fire-polished glass Pasteur pipette and gentle trituration, neurons were dissociated and dispersed in tcASW onto 35 × 10 mm polystyrene tissue culture dishes (353001, Falcon-Corning/ThermoFisher Scientific). Cultures were maintained in a 14°C incubator and used for experimentation within 1–3 d. Salts were obtained from ThermoFisher Scientific, MP Biomedicals, Acros Organics, or Sigma-Aldrich.

Whole-cell voltage-clamp and current-clamp recording from cultured bag cell neurons. Tight-seal, whole-cell recordings of membrane current or voltage from cultured bag cell neurons were performed at room temperature (20–22°C) using an EPC-8 amplifier (HEKA Electronik/Harvard Apparatus). Borosilicate-glass microelectrodes had a resistance of 1–2 MΩ when filled with various intracellular saline (see following paragraph). Pipette and membrane capacitive currents were cancelled and the series resistance (3–5 MΩ) compensated to 70–80%. Current was low-pass filtered at 1 kHz and sampled at 2 kHz using a Digidata 1322A analog-to-digital converter (Molecular Devices) and the Clampex acquisition program of pCLAMP v8.1 (Molecular Devices). Holding and test potentials (see Results) were delivered using pCLAMP. Voltage was low-pass filtered at 5 kHz and sampled as per current; in addition, membrane potential was initially set to −60 or −40 mV with constant bias current from the EPC-8.

Unless otherwise noted, most recordings were made in normal artificial sea water (nASW; composition as per tcASW but lacking glucose and antibiotics) with a Cs^+-based intracellular saline (composition in mM: 500 Cs^+-Asp, 70 KCl, 1.25 $MgCl_2$, 10 HEPES, 11 glucose, 10 glutathione, 5 EGTA, 5 adenosine 5′-triphosphate $2Na{\cdot}H_2O$ (A3377, Sigma-Aldrich), and 0.1 guanosine 5′-triphosphate $Na{\cdot}H_2O$ (G8877, Sigma-Aldrich), pH 7.3 with KOH. Some experiments used a K^+-based intracellular saline as per the Cs^+-based saline, but with K^+ replacing Cs^+. For both intracellular salines, as calculated using WebMaxC (https://somapp.ucdmc.ucdavis.edu/pharmacology/bers/maxchelator/webmaxc/webmaxcS.htm), 3.75 mM $CaCl_2$ was added to set the free Ca^{2+} concentration at 300 nM, which corresponds to the approximate resting intracellular Ca^{2+} concentration of bag cell neurons as determined using either Ca^{2+}-sensitive electrodes (Fisher et al., 1994) or imaging of Ca^{2+}-sensitive dyes (Fink et al., 1988; Loechner et al., 1992; Knox et al., 1996; Magoski et al., 2000). Junction potentials of 17 and 15 mV were calculated for the Cs^+-based and K^+-based intracellular salines, respectively, versus nASW and compensated for by subtraction off-line. In a small number of experiments, voltage-gated Ca^{2+} current was recorded by using the Cs^+-based intracellular saline and an ASW where all of the Na^+ and K^+ were replaced with tetraethylammonium and Cs^+, respectively. The 20 mV junction potential for this saline combination was compensated for by subtraction off-line.

Experiments designed to examine the reversal potentials of the H_2O_2-induced current involved external Na^+ and Ca^{2+} substitutions to make Na^+-free [composition as per nASW but with the Na^+ replaced by *N*-methyl-D-glucamine (NMDG)], Ca^{2+}-free (Ca^{2+} replaced by Mg^{2+}), and Na^+/Ca^{2+}-free (Na^+ replaced by NMDG and Ca^{2+} replaced by Mg^{2+}) salines. Junction potentials of 17 mV for Ca^{2+}-free

ASW and 23 mV for both Na^+-free ASW and Na^+/Ca^{2+}-free ASW versus the Cs^+-based intracellular saline were compensated for by subtraction off-line.

Ensemble extracellular recording from the intact bag cell neuron cluster. For extracellular recording, the abdominal ganglion, including the two bag cell neuron clusters and associated pleuroabdominal connectives, was isolated and maintained in nASW-filled dish kept at a 14°C by immersion in a water-cooled chamber. A wide-bore, fire-polished glass suction recording electrode (containing nASW) was placed over one of the two bag cell neuron clusters, while a similarly fashioned stimulating electrode was placed at the rostral end of the pleuroabdominal connective ipsilateral to the recorded cluster. Synaptic input was stimulated with current from a Grass SD9 stimulator (Astro-Med) while voltage was monitored with a Model 3000 AC/DC differential amplifier (A-M Systems). Voltage was high-pass filtered at 10 Hz and low-pass filtered at 1 kHz, and acquired at 2 kHz using AxoScope v9.0 (Molecular Devices) as per whole-cell voltage-clamp.

Sharp-electrode recording from bag cell neurons in culture and isolated clusters. Sharp-electrode recordings from bag cell neurons were performed using an AxoClamp 2B amplifier (Molecular Devices) at room temperature (20–22°C). Borosilicate-glass microelectrodes had a resistance of 5–20 MΩ when filled with 2 M K^+-acetate plus 10 mM HEPES and 100 mM KCl, pH 7.3 with KOH. Voltage-clamp was performed on single, cultured bag cell neurons using continuous single-electrode voltage-clamp at a holding potential of −30 mV. Whereas current-clamp was undertaken on bag cell neurons in desheathed, isolated clusters using the bridge-balance method. A Grass S88 stimulator was used to deliver 50 ms hyperpolarizing current pulses to balance the bridge; in addition, bias current was injected into the neuron as necessary from the AxoClamp. Current or voltage was filtered to 3 kHz before sampling at 2 kHz as per whole-cell voltage-clamp with Clampex.

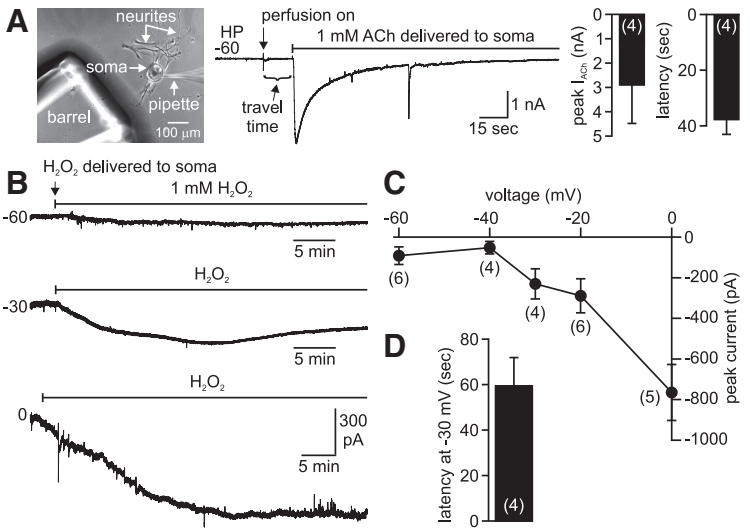

Figure 1. H_2O_2 activates a prolonged, inward, voltage-dependent current in cultured bag cell neurons. ***A***, Left, Phase-contrast photomicrograph showing a superfusion barrel positioned near a bag cell neuron soma with neurites and the recording pipette. Neurons are whole-cell voltage-clamped at −60 mV using our standard K^+-Asp-based intracellular saline in the pipette and nASW in the bath. Middle, Superfusion of 1 mM ACh (at bar) elicits an inward current. Arrows highlight the start of superfusion and travel time, i.e., the time required for ACh to reach the soma. Right, ACh superfusion produced a peak current (I_{ACh}) of −2.9 ± 1.6 nA with a latency of 38.0 ± 5.3 s following the switch from control to ACh-containing saline. ***B***, Superfusion of 1 mM H_2O_2 (at bar) over the soma of different neurons, held at −60, −30, or 0 mV, causes increasingly larger inward current. Ordinate applies to all traces. ***C***, Summary current/voltage relationship for the H_2O_2-induced current at −60 mV (91.0 ± 43 pA), −40 mV (51.0 ± 31.0 pA), −30 mV (230.0 ± 74.0 pA), −20 mV (288.0 ± 84.0 pA), or 0 mV (765.0 ± 138.0 pA), shows a threshold between −40 and −30 mV and an apparent maximum at 0 mV. ***D***, Group data illustrating a 59.9 ± 12.4 s latency of the H_2O_2-induced current at −30 mV.

Drug application and reagents. Solution exchanges were initially accomplished using a calibrated transfer pipette to replace the bath (culture dish) tcASW with the desired extracellular saline before the start of a given experiment. In most cases, drugs were introduced before or during recording by initially removing a small volume (~50 μl) of saline from the bath, combining that with an even smaller volume (<10 μl) of drug stock-solution (see following paragraph), and then reintroducing that mixture back into the bath. Care was taken to pipette near the side of the dish and as far away as possible from the neuron. For some experiments, drugs or transmitters were applied using a single-cell superfusion system consisting of a micromanipulator-controlled square-barreled glass pipette (~500 μm bore; 8250, VitroCom) positioned 300–500 μm from the soma and connected by a stopcock manifold to a series of gravity-driven reservoirs. This provided a constant flow (~0.5–1 ml/min) of control extracellular saline over the neuron, which was switched to drug-containing saline by activating the appropriate stopcock. The bath volume was kept constant during superfusion with vacuum-trap suction outlet.

Water was used to dissolve the following as stocks at the indicated concentrations: H_2O_2 0.2 M (H325–500, ThermoFisher Scientific), mercaptosuccinic acid (0.3 M; M6182; Sigma-Aldrich), acetylcholine chloride (ACh; 100 mM; A6625, Sigma-Aldrich), DL-dithiothreitol (DTT; 50 mM; 646563, Sigma-Aldrich), 1-(2-(3-(4-methoxyphenyl)propoxy)-4-methoxyphenylethyl)-1H-imidazole (SKF-96365; 50 mM; S7809, Sigma-Aldrich), tetrodotoxin (TTX; 3 mM; T-550, Alomone Labs), and *N*-acetyl-L-cysteine (NAC; 150 mM; A7250, Sigma-Aldrich). Similarly, dimethyl sulfoxide (DMSO; BP231-1, ThermoFisher Scientific) was used to dissolve the following: clotrimazole (25 mM; C6019, Sigma-Aldrich), and 9-phenanthrol (9-Pt; 50 mM; 211281, Sigma-Aldrich). Last, ethanol (100% v/v) was used to dissolve *N*-ethylmaleimide (NEM; 50 mM; E3876, Sigma-Aldrich). The final concentration of DMSO or ethanol in the bath was ≤0.2% (v/v), which in control experiments here or in prior studies was found to have no effect on bag cell neuron holding current, membrane conductance, or membrane potential (Hickey et al., 2010, 2013; Tam et al., 2011; Sturgeon and Magoski, 2016; White et al., 2018).

Analysis. The Clampfit analysis program of pCLAMP was used to determine the amplitude of changes to membrane current or potential evoked by H_2O_2 or other reagents under voltage- or current-clamp. For peak change, two cursors were placed 30 s apart, 30 s before drug addition, the average between the cursors served as a baseline. An additional two cursors were placed 60 s apart on either side of the peak of the response. Clampfit then calculated the peak amplitude relative to the baseline. Percent recovery of the current following a response was determined by comparing the peak current to the steady-state current, the latter being calculated by again placing two cursors, 30 s apart, at the end of the trace, well after the maximal response and where the response had recovered to steady-state. For display only, some current traces were filtered off-line to between 50 and 100 Hz using the Clampfit Gaussian filter. Due to the overall slow nature of the responses, this second filtering brought about no change in amplitude or kinetics. Conductance was derived using Ohm's law ($G = I/V$) and the current change during a 200 ms step from −30 to −40 mV before and after H_2O_2. Reversal potential involved taking a difference current, ascertained by subtracting the current elicited by a voltage ramp from −60 to +60 mV before H_2O_2 superfusion, from the current elicited by the same ramp at the peak of the H_2O_2-induced current. The reversal potential was then measured directly from the difference current by placing a cursor where the current crossed the *y*-axis. For some responses recorded under current-clamp that presented with robust spiking, which made it difficult to visualize the peak depolarization, Clampfit was used to generate all-point histograms for before and after H_2O_2 application. The largest peaks of the resulting histograms were fit with a Gaussian function by the least-squares method and a simplex search, and taken as the average membrane potential. The

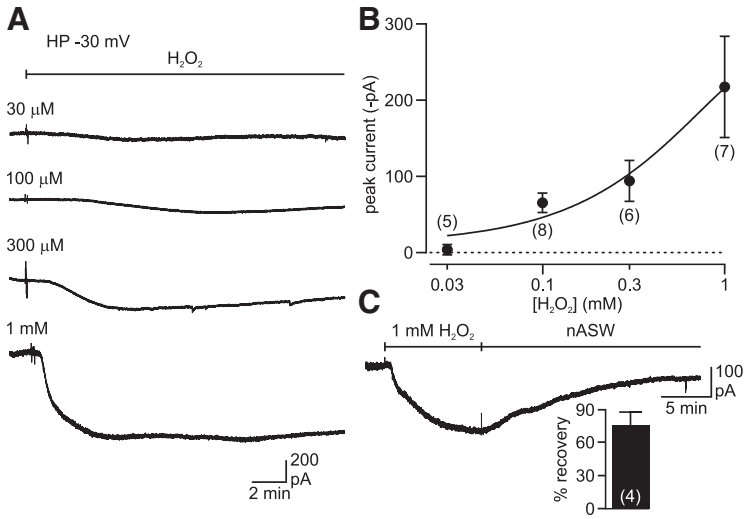

Figure 2. A concentration-dependent H_2O_2-induced inward current. ***A***, Current responses to bath-applied 30 μM, 100 μM, 300 μM, or 1 mM H_2O_2 (at bar) for different cultured bag cell neurons whole-cell voltage-clamped at −30 mV in nASW with Cs^+-Asp-based intracellular saline. Scale bars apply to all traces. ***B***, Concentration–response curve reveals increasingly higher amounts of H_2O_2 induces progressively larger currents (30 μM = 4.0 ± 7.0 pA, 100 μM = 66.0 ± 13.0 pA, 300 μM = 94.0 ± 27.0 pA, 1 mM H_2O_2 = 218.0 ± 66.0 pA). The line represents the fit of the data with a four-parameter dose–response equation, and provides an EC_{50} of 14.2 mM with a Hill slope of 0.64. ***C***, Upon washout of 1 mM H_2O_2 with nASW, at the height of the response, the current recovered largely back to the baseline. Inset, Summary graph shows 73.0 ± 10.6% recovery, calculated by comparing the baseline (before H_2O_2 superfusion) and the stable current at end of the trace.

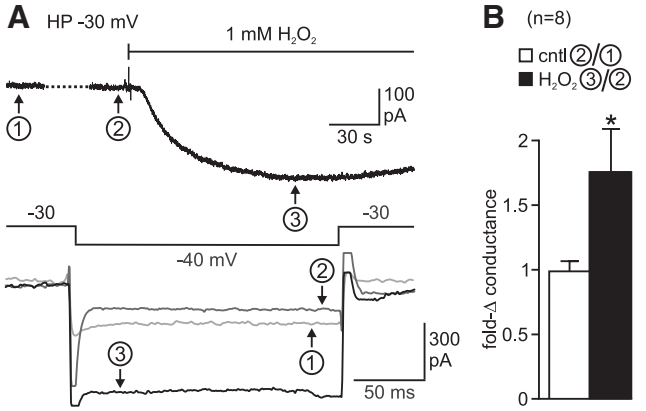

Figure 3. H_2O_2 increases membrane conductance. ***A***, Top, Typical example of 1 mM H_2O_2 superfusion (at bar) evoking a current in a bag cell neuron whole-cell voltage-clamped at −30 mV in nASW using Cs^+-based intracellular saline. Middle, To determine membrane conductance, a 200 ms step to −40 mV is given ~90 s before H_2O_2 (arrow, circled 1). A second step is taken right before H_2O_2 delivery (circled 2), whereas a third step is taken at the peak of the response (circled 3). Bottom, The current evoked by the step is markedly elevated at the peak of the H_2O_2 current (3; black trace) compared with that taken immediately (2; dark gray) or ~90 s before H_2O_2 (1; light gray). ***B***, Summary graph shows a significant increase in fold-change conductance, calculated by obtaining the ratios of the step-current taken just before H_2O_2 superfusion versus ~90 s earlier (control 2/1 = 1.0 ± 0.079) and during H_2O_2 versus just before superfusion (H_2O_2 3/2 = 1.7 ± 0.33; r = 0.02381; *p = 0.0078, Wilcoxon matched-pairs signed ranks test).

difference between the voltage before and after H_2O_2 served as the amplitude of the depolarization. To determine the frequency of firing caused by H_2O_2, the number of spikes during the response was determined using the Clampfit threshold search function, and was divided by the total time of the burst (in seconds) to derive action potential frequency.

Experimental design and statistical analysis. Data are mean ± SEM. Statistical analysis was performed using InStat v3.10 and Prism v8.0.0. The Kolmogorov–Smirnov method was used to test for normality. To test whether the mean differed between two groups of normally distributed data, Student's unpaired t test with Welch correction as necessary was used, whereas for not normally distributed data, the Mann–Whitney U test or Wilcoxon matched-pairs signed ranks test was used. For three or more means, normally distributed data were compared using an ordinary one-way ANOVA followed by the Tukey-Kramer multiple-comparisons test or Dunnett multiple-comparisons test, whereas not normally distributed data were compared using a Kruskal–Wallis ANOVA (KW-ANOVA) followed by Dunn's multiple-comparisons test. Significance level was a two-tailed p value of < 0.05. Prism was also used to fit the H_2O_2 concentration–response relationship with a four-parameter dose–response equation to determine the half-maximal concentration (EC_{50}) and the Hill slope (steepness of the curve).

Results

H_2O_2 activates a prolonged, inward voltage-dependent current in cultured bag cell neurons

H_2O_2 has been shown to induce changes in the excitability of sensory neurons in *Aplysia*, as well as striatal, substantia nigra, spinal ventral horn, hippocampal, or cortical neurons (Chen et al., 2001; Chang et al., 2003; Olah et al., 2009; Lee et al., 2011, 2013; Ohashi et al., 2016). Given that PKC, which is upregulated 2–5 min from the onset of the afterdischarge (Wayne et al., 1999), can increase H_2O_2 production in bag cell neurons (Munnamalai et al., 2014), we examined the effects of extracellularly applied H_2O_2 on bag cell neurons in primary culture.

Initially, the efficacy of the superfusion apparatus was assessed to ascertain the exact time of H_2O_2 delivery to the neuron. This involved superfusing (see Materials and Methods, Drug application and reagents) 1 mM ACh over the soma of a neuron under whole-cell voltage-clamp at −60 mV (Fig. 1*A*, left). We previously established that ACh gates, with essentially no delay, an ionotropic receptor in bag cell neurons (White and Magoski, 2012). This ligand-gated channel opens as soon as ACh contacts the cell, and is sensitive to classic nicotinic-type agonists and antagonists (White and Magoski, 2012; White et al., 2014). Thus, the latency from when the ACh-containing reservoir was opened to when the ACh-induced current was first observed represented the lag time of our perfusion apparatus.

Neurons were bathed in Na^+-containing nASW and dialyzed for 15 min with our standard K^+-Asp-based intracellular saline (see Materials and Methods, Whole-cell voltage-clamp and current-clamp recording from cultured bag cell neurons). ACh induced an inward current of ~3 nA with a mean onset latency of 38 ± 5.3 s (n = 4) from the time superfusion began, i.e., when the stopcock on the reservoir was switched (Fig. 1*A*, middle, right). Subsequently, it was assumed that when H_2O_2 was superfused it took 38 s to reach the soma. Parenthetically, we performed a second calibration using block of voltage-gated Ca^{2+} current by 10 mM Ni^{2+}, which inhibits the Ca^{2+} current almost instantly (Hung and Magoski, 2007). Ca^{2+} current was evoked at a frequency of 1 Hz using a 75 ms step from −60 to 0 mV; when the perfusion was switched from control saline to Ni^{2+}-containing saline, it required 40 ± 3.5 s for Ni^{2+} to initiate block (n = 10). This lag time was not significantly different from that observed

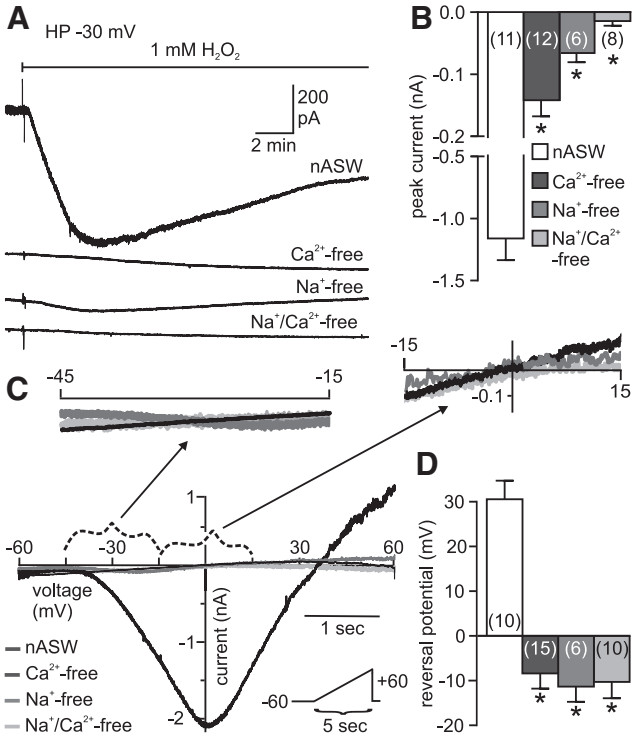

Figure 4. The H_2O_2-induced current is sensitive to change in extracellular cations. ***A***, Different individual cultured bag cell neurons under whole-cell voltage-clamp at −30 mV using Cs^+-based intracellular saline. Compared with the current elicited by 1 mM H_2O_2 (at bar) in Na^+-containing nASW, the response is smaller in Ca^{2+}-free or Na^+-free saline, and mostly eliminated in Na^+/Ca^{2+}-free saline. Scale bars apply to all traces. ***B***, Group data show that, in contrast to nASW (1.2 ± 0.2 nA), Ca^{2+}-free (151.6 ± 26.4 pA), Na^+-free (65.3 ± 15.3 pA), or Na^+/Ca^{2+}-free saline (14.1 ± 7.6 pA) all significantly reduce the current ($H = 29.991$; df = 2; $p < 0.0001$, KW-ANOVA; *$p < 0.05$ nASW vs Ca^+-free; *$p < 0.01$ nASW vs Na^+-free; *$p < 0.001$, nASW vs Na^+/Ca^{2+}-free, Dunn's multiple-comparisons test). ***C***, Difference currents obtained by subtracting the response to a 5 s, −60 to +60 mV voltage ramp (bottom inset), taken immediately before 1 mM H_2O_2 application, from that taken at the peak of the response. For nASW (black trace), the current is voltage-dependent and reverses between +30 and +40 mV. Upper insets show magnified Ca^{2+}-free (dark gray), Na^+-free (medium gray), and Na^+/Ca^{2+}-free (light gray) difference currents from −45 to −15 mV (left) and −15 to +15 mV (right). ***D***, Average data illustrates a significant left-shift in reversal potential from nASW (30.6 ± 4.1 mV) with Ca^{2+}-free (−8.4 ± 3.4 mV), Na^+-free (−11.3 ± 3.4 mV), or Na^+/Ca^{2+}-free (−10.3 ± 3.7 mV) saline ($F_{(3,37)} = 27.329$; $p < 0.0001$, ordinary ANOVA; *$p < 0.01$, nASW vs Ca^{2+}-free, nASW vs Na^+-free, and nASW vs Na^+/Ca^{2+}-free saline, Dunnett multiple-comparisons test). Bars as per panel ***B***.

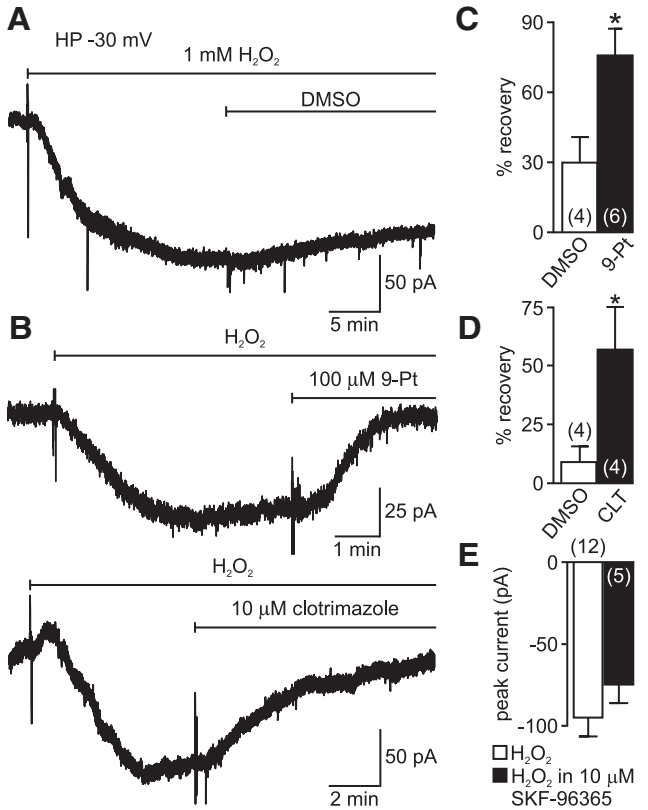

Figure 5. The pharmacology of the H_2O_2-induced current is consistent with a cation channel. ***A***, Whole-cell voltage-clamp recording from a cultured bag cell neuron in nASW at −30 mV using Cs^+-Asp-based intracellular saline shows an inward current in response to 1 mM H_2O_2 (at bar). Bath-application of 0.1% (v/v) DMSO (vehicle, at second bar) at the peak of the response fails to alter the normal recovery of the current. ***B***, Delivery of 100 μM 9-Pt (top) or 10 μM clotrimazole (bottom) at the peak of the response markedly inhibits the ongoing 1 mM H_2O_2-induced current. ***C***, ***D***, Summary graphs show both 9-Pt and clotrimazole significantly increase the percent recovery of the H_2O_2-induced current to 76.0 ± 11.4% and 56.5 ± 14.1%, respectively, calculated by comparing the baseline (before H_2O_2 bath-application) and the steady-state current at the end of the trace ($t_{(8)} = 2.743$; *$p = 0.0253$, 9-Pt, $t_{(6)} = 3.183$; *$p = 0.0190$, clotrimazole, both unpaired Student's *t* test). ***E***, Group data of the H_2O_2-induced current in control vs neurons pretreated with 10 μM SKF-96365. In contrast to 1 mM H_2O_2 alone (93.4 ± 11.4 pA), the presence of 10 μM SKF-96365 (73.3 ± 11.2 pA) does not significantly reduce the response ($U_{(5,12)} = 21.0$; $p = 0.3827$ H_2O_2 vs H_2O_2 in SKF-96365; Mann–Whitney *U* test).

for response onset of the ACh-induced current ($t_{(12)} = 0.3097$; $p = 0.7621$, unpaired Student's *t* test).

Superfusion of 1 mM H_2O_2 dissolved in nASW while holding the membrane potential at −60, −40, −30, −20, or 0 mV elicited a voltage-dependent inward current (Fig. 1*B*). There was minimal current (<100 pA) at −60 mV ($n = 6$) or −40 mV ($n = 4$), whereas more moderate currents (200–300 pA) were evoked at −30 ($n = 4$) or −20 mV ($n = 6$), with the maximal current (~800 pA) at 0 mV ($n = 5$; Fig. 1*C*). At −30 mV, the latency from when H_2O_2 arrived at the cell to when the current began was ~60 s ($n = 4$; Fig. 1*D*).

A concentration-dependent H_2O_2-induced inward current

To assess the sensitivity of bag cell neurons to H_2O_2, we examined the effect of various concentrations. Previous reports, using both vertebrate and invertebrate neurons, used a range of H_2O_2 from 1 to 3 mM, which did not cause damage in the short-term (Chen et al., 2001; Chang et al., 2003; Olah et al., 2009; Lee et al., 2011, 2013; Ohashi et al., 2016). Additionally, limitations on membrane permeability and intracellular scavenging suggests that the H_2O_2 concentration inside a cell is at least tenfold (perhaps even 650-fold) less than the concentration of extracellularly applied H_2O_2 (Antunes et al., 2000; Miller et al., 2007; Huang and Sikes, 2014).

Because the H_2O_2-induced current was rather small at −60 mV, and the holding current was often not entirely stable at 0 mV, we chose to examine the response at −30 mV in subsequent recordings. This provided a more uniform H_2O_2-induced current with a reasonably stable baseline. Cultured bag cell neurons were whole-cell voltage-clamped in nASW using a Cs^+-Asp-based intracellular saline to block K^+ channels and further improve resolution at this somewhat depolarized potential (Colmers et al., 1982; see Materials and Methods, Whole-cell voltage-clamp and current-clamp recording from cultured bag cell neurons). H_2O_2 was tested at 30 μM, 100 μM, 300 μM, and 1 mM ($n = 5, 8, 6, 7$). The resulting inward current was concentration-dependent, with a threshold of 100 μM and the largest response at 1 mM (Fig. 2*A*,*B*). Fitting the concentration-response relation-

ship with a four-parameter dose–response equation yielded an apparent EC_{50} of 14.2 mM with a Hill slope of 0.64. If this was due to an agonist-type mechanism, it would be expected that the H_2O_2-induced current would recover following drug removal. When the H_2O_2-containing nASW superfusing over the soma was replaced with nASW alone, shortly after the H_2O_2-induced current reached peak, it recovered by ~75% ($n = 4$; Fig. 2*C*, inset).

The H_2O_2-induced current is consistent with the opening of a nonselective cation channel

To verify channel opening, the membrane conductance was examined before and after H_2O_2 application, by delivering a 200 ms step to −40 mV from a holding potential of −30 mV under voltage-clamp (Fig. 3*A*, middle). A first step was delivered after a 15 min dialysis period, while a second step was given ~90 s after that, right before 1 mM H_2O_2 superfusion, and a third step was performed at the peak of the H_2O_2 response (Fig. 3*A*, top). The ratios of the current from the second step (just before H_2O_2) versus the first step (Fig. 3*B*, control 2/1), and the third step (at the peak of H_2O_2 response) versus second step (Fig. 3*B*, H_2O_2 3/2) were taken to ascertain the change in conductance. The period preceding H_2O_2 presented essentially no change in conductance (~0.99-fold); however, the conductance change at the peak of the H_2O_2 response was significantly larger (by ~1.75-fold), in agreement with channel opening ($n = 8$; Fig. 3*A*, bottom, *B*).

We next characterized the ionic basis of the current. The permeability of Na^+ and Ca^{2+} was studied by replacing extracellular Na^+ with NMDG and/or Ca^{2+} with Mg^{2+} (see Materials and Methods, Whole-cell voltage-clamp). Compared with nASW as control ($n = 11$), the H_2O_2-induced current was reduced by ~87% in Ca^{2+}-free ($n = 12$), ~95% in Na^+-free ($n = 6$), and was almost absent in Na^+/Ca^{2+}-free ($n = 8$) extracellular saline (Fig. 4*A*), suggesting that H_2O_2 acts on a nonselective cation conductance. On average, the observed decreases in current were significant versus control (Fig. 4*B*).

Ion substitution was also used to investigate the reversal potential of the H_2O_2-induced current. Specifically, a 5 s ramp from −60 to +60 mV was delivered under voltage-clamp from a holding potential of −30 mV (Fig. 4*C*). The ramp was given twice, i.e., right before H_2O_2 application, and again at the peak of the H_2O_2 response. A difference current was then calculated by subtracting the first ramp-induced current from the second ramp-induced current. In nASW, the difference current was nonlinear (inward between ~−30 and ~+30 mV), voltage-dependent, and reversed at ~+30 mV ($n = 10$; Fig. 4*C*). However, in the absence of extracellular Ca^{2+}, or Na^+, or Na^+/Ca^{2+}, the difference currents flattened out (Fig. 4*C*, top insets). Moreover, the reversal potential was significantly left-shifted in Ca^{2+}-free (~−8 mV; $n = 15$), Na^+-free (~−11 mV; $n = 6$), or Na^+/Ca^{2+}-free saline (~−10 mV; $n = 10$), as expected for a nonselective cation conductance (Fig. 4*D*).

The pharmacology of the H_2O_2-induced current is also consistent with a cation channel

Because the ion substitution and reversal potential results suggested a nonselective cation channel, we subsequently tested known cation channel blockers. In particular, 9-Pt, a purported transient receptor potential (TRP) cation channel melastatin subfamily isoform 4-specific inhibitor (Grand et al., 2008; Guinamard et al., 2014), clotrimazole, a general cation channel blocker known to prevent H_2O_2-induced currents in striatal and hippocampal neurons (Hill et al., 2004; Olah et al., 2009), and

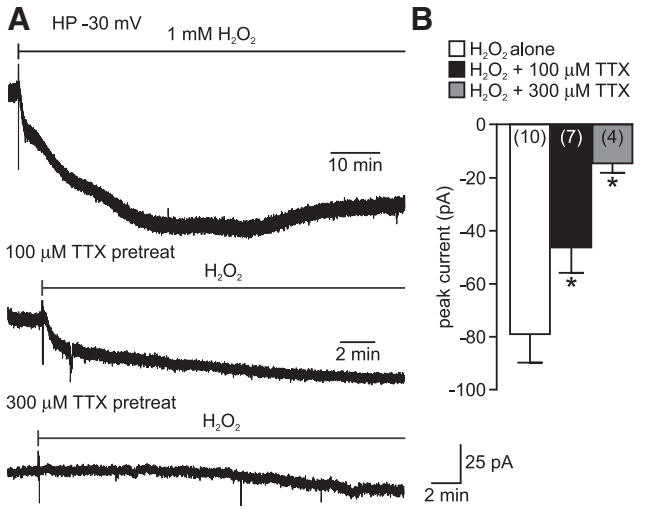

Figure 6. The H_2O_2-induced current is reduced by tetrodotoxin. ***A***, Current responses to 1 mM H_2O_2 (at bar) of separate cultured bag cell neurons whole-cell voltage-clamped at −30 mV in nASW with Cs^+-based intracellular saline. Compared with control (top), a 30 min pretreatment with 100 μM TTX (middle) noticeably reduces the H_2O_2-induced current, while 300 μM, TTX (bottom) almost eliminates the response. Ordinate applies to all traces. ***B***, Group data of the H_2O_2-induced current in 100 or 300 μM TTX vs control. Compared with 1 mM H_2O_2 alone (79.9 ± 7.7 pA), the presence of 100 μM (47.1 ± 9.4 pA) or 300 μM TTX (15.4 ± 3.6 pA) significantly reduces the response ($F_{(2,18)} = 12.570$; $p = 0.0004$ ordinary ANOVA, *$p < 0.05$ H_2O_2 vs H_2O_2 post 100 μM TTX; *$p < 0.01$ H_2O_2 vs H_2O_2 post 300 μM TTX, Dunnett multiple-comparisons test).

SKF-96365, which is often reported as a TRP channel canonical subfamily antagonist (Zhu et al., 1998), were used. Either 9-phenanthrol or clotrimazole were given at the peak of the response to 1 mM H_2O_2, the prediction being that a blocker would inhibit the channel and, compared with the vehicle (DMSO), increase the percent-recovery of the current (see Materials and Methods, Analysis). Whereas DMSO application (the vehicle; $n = 4, 4$) resulted in 10–30% recovery (Fig. 5*A*,*C*), introducing 100 μM 9-phenanthrol ($n = 6$) or 10 μM clotrimazole ($n = 4$; Fig. 5*B*, top, bottom), significantly increased the percent-recovery of the H_2O_2-induced current to ~75 and ~55%, respectively (Fig. 5*C*,*D*). For SKF-96365, 10 μM of the blocker was bath-applied 10 min before 1 mM H_2O_2 delivery; however, compared with H_2O_2 alone, the presence of SKF-96365 did not significantly alter the current (Fig. 5*E*).

Some TRPC channels are sensitive to changes in glucose concentration; for example, Lee et al. (2015b) reported that low glucose enhances neuronal TRPC channels, likely through a pathway involving the triggering of adenosine monophosphate-activated protein kinase. In the present study, the extracellular saline normally did not contain glucose (see Materials and Methods, Whole-cell voltage-clamp and current-clamp recording from cultured bag cell neurons); thus, we examined whether introducing 1 mM extracellular glucose beforehand would impact the H_2O_2-induced current. The presence of this low glucose concentration did not significantly alter the response to 1 mM H_2O_2 (H_2O_2 alone: 65.3 ± 16.0 pA, $n = 4$ vs H_2O_2 in glucose: 68.0 ± 16.7 pA, $n = 4$; $t_{(6)} = 0.1189$; $p = 0.9093$, unpaired Student's t test). Because the Cs^+-based intracellular saline used for most whole-cell experiments contained 11 mM glucose, we also performed a control for this intracellular addition of glucose via the pipette by recording the H_2O_2-induced current using sharp-electrode voltage-clamp. Neurons were impaled with a sharp-electrode (which does not permit appreciable exchange with the

cytosol) and held at −30 mV (see Materials and Methods, Sharp-electrode recording from bag cell neurons in culture and isolated clusters). We found that the current under the sharp-electrode configuration (140 ± 39.2 pA; $n = 6$) was not significantly different from parallel controls performed using whole-cell pipettes containing Cs^+-based intracellular saline with glucose (112 ± 32.2 pA; $n = 5$; $t_{(9)} = 0.5390$; $p = 0.6030$, unpaired Student's t test).

Our data suggest that the H_2O_2-induced current is mediated by a conductance similar to the voltage-dependent nonselective cation channel characterized in bag cell neurons by Wilson et al. (1996). Those authors reported that this channel was blocked by relatively high concentrations (80–100 μM) of the classical Na^+ channel antagonist, TTX (Narahashi et al., 1964). Thus, to confirm any similarity, we initially bath-applied 100 μM TTX at the peak of H_2O_2-induced current. However, we observed no difference in percent-recovery of the response in the presence ($n = 5$; 41.6 ± 7.7%) or absence of TTX ($n = 6$; 41.2 ± 8.6%; $t_{(9)} = 0.03097$; $p = 0.9760$, unpaired Student's t test). TTX has one primary alcohol and three secondary alcohol functional groups. Chicheportiche et al. (1980) showed that the secondary alcohols can be oxidized, resulting in inactive toxin. Thus, in the present study TTX may have been oxidized upon bath-application in the presence of H_2O_2. To avoid this, we opted for pretreatment with TTX and delivering H_2O_2 afterward. Compared with the control H_2O_2-induced current ($n = 10$), a 30 min pretreatment with 100 μM TTX ($n = 7$) reduced the response by ~40% (Fig. 6A, top, middle). Moreover, a further decrease in the response, to ~15% of control, was seen with 300 μM TTX pretreatment ($n = 4$; Fig. 6A, bottom). The presence of 100 or 300 μM TTX significantly reduced the H_2O_2 response versus control (Fig. 6B).

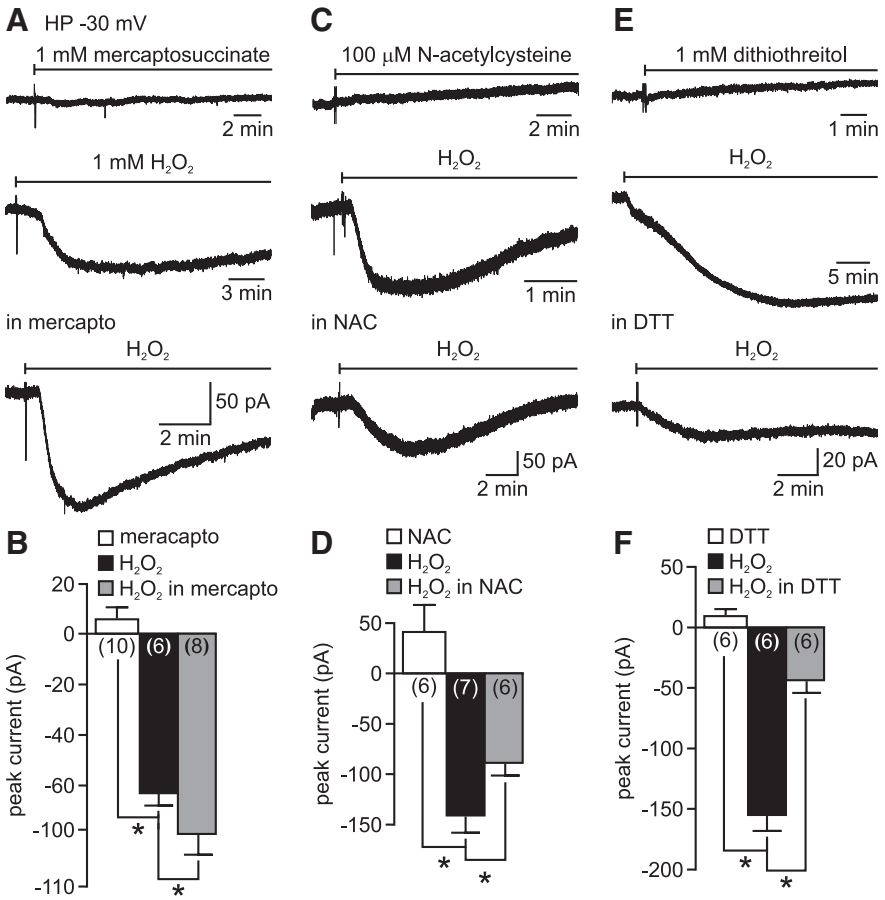

Figure 7. The H_2O_2-induced current is enhanced by mercaptosuccinate and reduced by *N*-acetylcysteine or dithiothreitol. Cultured bag cell neurons are bathed in nASW and whole-cell voltage-clamped at −30 mV using Cs^+-based intracellular saline. ***A***, Bath-application (at bar) of 1 mM mercaptosuccinate alone has little effect (top), whereas delivery of 1 mM H_2O_2 to a second cell elicits a noticeable inward current (middle). Moreover, in a third neuron initially given mercaptosuccinate (mercapto), the H_2O_2-induced current is enhanced by ~50% (bottom). Ordinate applies to all traces. ***B***, Summary graph of peak mercaptosuccinate- and H_2O_2-induced current ± mercaptosuccinate. There is a significant difference between both the H_2O_2-induced current with (98.1 ± 9.6 pA) and without (66.4 ± 5.8 pA) mercaptosuccinate as well as mercaptosuccinate alone (7.3 ± 7.2 pA; $F_{(2,21)} = 50.879$; $p < 0.0001$, ordinary ANOVA; *$p < 0.001$ mercapto vs H_2O_2; *$p < 0.05$ H_2O_2 vs H_2O_2 in mercapto, Tukey–Kramer multiple-comparisons test). ***C***, Introducing 100 μM NAC has only a nominal impact (top), whereas 1 mM H_2O_2 generates an inward current (middle). In the presence of *N*-acetylcysteine, the H_2O_2-induced current is reduced by ~40% (bottom). ***D***, Summary data showing that compared with *N*-acetylcysteine alone (43.3 ± 25.7 pA), the H_2O_2-induced current differs significantly with (90.3 ± 21.4 pA) and without *N*-acetylcysteine (148.0 ± 16.0 pA; $U_{(6,7)} = 0$; *$p = 0.0034$ NAC vs H_2O_2; $U_{(6,7)} = 5$; *$p = 0.0221$ H_2O_2 vs H_2O_2 in NAC, both Mann–Whitney *U* test). ***E***, Minimal response to 1 mM DTT alone (top), whereas 1 mM H_2O_2 again elicits a clear inward current (middle); in addition, when DTT is already present, the H_2O_2-induced current is reduced by ~70% (bottom). ***F***, Group data showing that compared with DTT alone (11.3 ± 4.5 pA), the H_2O_2-induced current differs significantly with (43.2 ± 9.6 pA) and without DTT (155.0 ± 13.2 pA; $F_{(2,15)} = 73.831$; $p < 0.0001$, ordinary ANOVA; *$p < 0.001$ DTT vs H_2O_2; *$p < 0.001$ H_2O_2 vs H_2O_2 in DTT, Tukey–Kramer multiple-comparisons test).

The H_2O_2-induced current is boosted by preventing oxidation and attenuated by promoting reduction

Glutathione peroxidase is a cytosolic enzyme that catalyzes the reduction of H_2O_2 to H_2O, and the concomitant oxidation of glutathione (Jones et al., 1981). Mercaptosuccinate inhibits glutathione peroxidase, thus preventing H_2O_2 reduction (Dringen et al., 1998); hence, we hypothesized that delivering mercaptosuccinate for ~10 min before H_2O_2 would increase the response. Bath-application of 1 mM mercaptosuccinate alone had little to no effect on the holding current ($n = 10$; Fig. 7A, top). As expected, introducing 1 mM H_2O_2 on its own ($n = 6$) produced an inward current; in addition, this was significantly enhanced by ~50% in the presence of mercaptosuccinate ($n = 8$; Fig. 7A, middle, bottom, B). To further examine the role of glutathione in moderating the H_2O_2-induced current, we initially exposed neurons to 100 μM of *N*-acetylcysteine, which increases glutathione levels by elevating the intracellular concentration of the glutathione synthesis precursor, cysteine (Cotgreave et al., 1991). On its own, *N*-acetylcysteine did not cause a change in current at −30 mV ($n = 6$; Fig. 7C, top); yet, delivery of 1 mM H_2O_2 ~10 min after *N*-acetylcysteine ($n = 6$) evoked an inward current which was significantly reduced by ~40% when contrasted with the response to just H_2O_2 ($n = 7$; Fig. 7C, middle, bottom, D).

To test whether cation channel activation by H_2O_2 occurs via oxidation of sulfhydryl groups, we used DTT, a reducing agent that maintains thiol groups on amino acids, such as Cys, in the reduced state (Cleland, 1964). Application of DTT alone did not

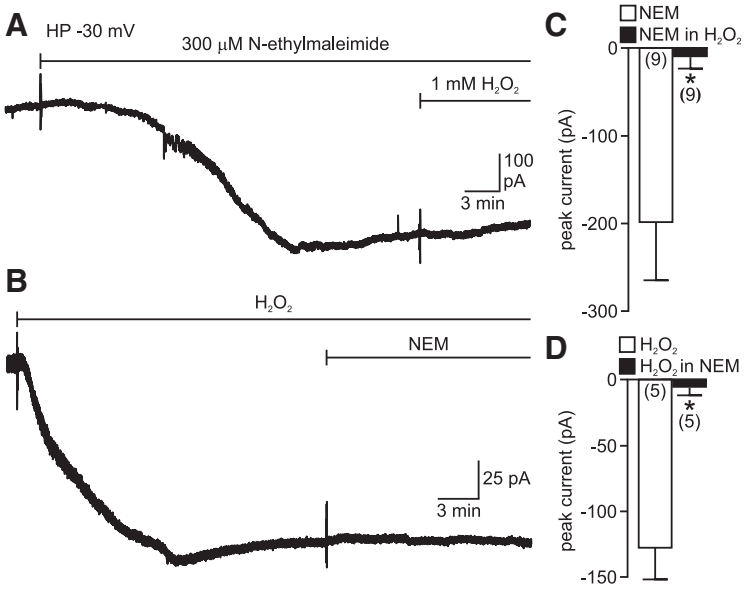

Figure 8. NEM- and H_2O_2-induced currents are occlusive. Representative response to 300 μM NEM or 1 mM H_2O_2 of different cultured bag cell neurons whole-cell voltage-clamped at −30 mV in nASW with Cs^+-based intracellular saline. ***A***, Bath-application (at bar) of NEM evokes a prominent inward current. Yet, H_2O_2 (at second bar) in the presence of NEM, yields little further change. ***B***, Delivery of H_2O_2 elicits a typical inward current in a separate neuron, but there is no obvious current when NEM is applied in the presence of H_2O_2. ***C***, ***D***, Summary data demonstrates a significant difference between the NEM-elicited current (201.0 ± 65.5 pA) and the H_2O_2-induced current post-NEM (11.7 ± 13.1 pA; $U_{(9,9)} = 7.0$; $^*p = 0.0019$, Mann–Whitney *U* test). Similarly, there is a significant difference between the H_2O_2-induced current (129.6 ± 24.5 pA) and the NEM-elicited current post-H_2O_2 (6.3 ± 5.9 pA; ($t_{(4)} = 4.90$; $^*p = 0.008$, unpaired Student's *t* test, Welch corrected). Note, there is no statistical difference between the initial current produced by NEM and H_2O_2 (white bars; $t_{(9)} = 1.022$; $p = 0.3337$, unpaired Student's *t* test, Welch corrected); as well, the NEM- and the H_2O_2-induced currents in the presence of H_2O_2 and NEM, respectively, are not statistically different (black bars; $U_{(5,9)} = 14.0$; $p = 0.2977$, Mann–Whitney *U* test).

elicit a current at −30 mV ($n = 6$; Fig. 7*E*, top). However, in the presence of DTT, the response to 1 mM H_2O_2 was obviously decreased compared with the delivery of H_2O_2 alone ($n = 6$; Fig. 7*E*, middle, bottom). The H_2O_2 current was reduced by ~70% and this drop was significant (Fig. 7*F*).

NEM- and H_2O_2-induced currents are occlusive

The ability of DTT to prevent H_2O_2 from activating the current suggests that H_2O_2 may gate the cation channel by direct oxidation of sulfur-containing amino acids, in particular, Cys and/or Met residues in the channel or an associated protein(s) (Hoshi and Heinemann, 2001). NEM is a sulfydryl alkylating agent (Jakobs et al., 1982) that can remove hydrogen from thiol side chains and replace it with a carbon–sulfur bond, potentially minimizing H_2O_2-mediated oxidation (Gregory, 1955). Therefore, we tested the effects of NEM on both membrane current itself and the H_2O_2-induced current. Bath-application of 300 μM NEM elicited an ~200 pA inward current at −30 mV ($n = 9$), with the subsequent addition of 1 mM H_2O_2 evoking only a small response of ~12 pA ($n = 9$; Fig. 8*A*). Similarly, when H_2O_2 was added to the bath first, it brought about a typical inward current ($n = 5$), whereas delivery of NEM afterward again caused little change ($n = 5$; Fig. 8*B*). The currents induced by H_2O_2 and NEM, respectively, were not significantly different on average (Fig. 8*C*,*D*, two white bars); moreover, the two currents occluded one another (Fig. 8*C*,*D*, two black bars).

H_2O_2 depolarizes and induces robust action potential firing

Given that H_2O_2 application elicits an inward current, we sought to determine the impact of introducing H_2O_2 on cultured bag cell neuron membrane potential. This was performed using whole-cell current-clamp in nASW with the K^+-based intracellular saline in the pipette. H_2O_2 was tested at both −40 mV, the approximate membrane potential during the afterdischarge, and −60 mV, the approximate membrane potential before or at the start of the afterdischarge (Kupfermann and Kandel, 1970; Kaczmarek et al., 1982). Bath application of 100 μM H_2O_2 induced a depolarization of ~7 and ~14 mV from −40 ($n = 7$) and −60 mV ($n = 5$), respectively, versus H_2O as control at −40 mV ($n = 5$) or −60 mV ($n = 5$), which had no obvious effect (Fig. 9*A*,*B*). In no case did 100 μM H_2O_2 cause the neuron to fire action potentials. However, 1 mM H_2O_2 not only depolarized the membrane, by ~11 mV for −40 mV ($n = 5$) and ~22 mV for −60 mV ($n = 5$), but consistently evoked a burst of spikes (Fig. 9*C*). Compared with H_2O, the magnitudes of the responses were significant for both −40 and −60 mV (Fig. 9*D*). As for the action potential firing, it lasted for ~8 min at −40 mV and ~7 min at −60 mV with the latency of ~3 min and frequency of ~1 Hz at both voltages (Fig. 9*E*).

Knowing that the H_2O_2-induced current is blocked by 9-phenanthrol, clotrimazole, or TTX, we next investigated whether these blockers altered the depolarization to 1 mM H_2O_2 from −40 mV. As expected, 1 mM H_2O_2 ($n = 18$) elicited a depolarization of ~9 mV and action potential firing of ~1 Hz that lasted for ~12 min (Fig. 10*A*, top, *B*). This response was essentially eliminated by a 20 min pretreatment with either 10 μM clotrimazole ($n = 6$; −2.8 ± 1.4 mV) or 100 μM 9-phenanthrol ($n = 6$; 4.0 ± 2.2 mV; Fig. 10*A*, middle). As for TTX ($n = 4$), incubating in 300 μM did not prevent the depolarization altogether (Fig. 10*B*, top); instead, it significantly reduced the firing frequency to ~0.5 Hz and the duration of spiking to ~3 min (Fig. 10*A*, bottom, *B*, middle, bottom).

H_2O_2 depolarizes bag cell neurons and initiates an afterdischarge in desheathed clusters

Because H_2O_2 both gates a cation channel and causes bursting in cultured bag cell neurons, we sought to ascertain whether H_2O_2 can produce afterdischarge-like responses from the bag cell neuron cluster itself. To begin with, 1–10 mM H_2O_2 was bath-applied to the entire abdominal ganglion while recording extracellularly from one of the two intact bag cell neuron clusters (see Materials and Methods, Ensemble extracellular recording from the intact bag cell neuron cluster). However, this failed to bring about an afterdischarge nor did H_2O_2 affect the ability of synaptic input to evoke an afterdischarge, as subsequent stimulation of the pleuroabdominal connective resulted in normal afterdischarges that were of the same duration ($n = 4$; 57.8 ± 12.6 min) compared with those elicited in ganglia not exposed to H_2O_2 ($n = 7$; 44.4 ± 14.1 min; $t_{(9)} = 0.6349$; $p = 0.5413$, unpaired Student's *t* test).

It is possible that the sheath surrounding the cluster hindered diffusion of H_2O_2 to the bag cell neurons and/or antioxidant mechanisms present either in the sheath cells or the extracellular space reduced the exogenous H_2O_2. Therefore, to demonstrate

that direct delivery of H_2O_2 to the cluster can elicit bursting, the connective sheath was removed and the entire bag cell neuron cluster was isolated from the abdominal ganglion and placed in a culture dish. Sharp-electrode recordings were then made within the cluster from individual bag cell neurons initially current-clamped at −60 mV (see Materials and Methods, Sharp-electrode recording from bag cell neurons in culture and isolated clusters). Still, bath-applying 10 mM H_2O_2 alone resulted in a depolarization of just ~10 mV ($n = 5$; Fig. 11*C*, left, white bar), with only one of the five preparations exhibiting a 10.9 min burst of action potentials.

We speculated that H_2O_2 may need to work in concert with the known bag cell neuron input transmitter, ACh (White and Magoski, 2012). Previously, our lab showed that brief pressure-application of ACh to the isolated bag cell neuron cluster would initiate a transient depolarization in a given neuron, sometimes accompanied by afterdischarge-like spiking (White et al., 2018). Thus, in the present study, while again recording from a single bag cell neuron within the cluster, ACh was first pressure-ejected followed by the introduction of H_2O_2 (Fig. 11*B*, inset). In nine separate preparations, a 2 s pressure-ejection of 1 mM ACh to one side of the cluster caused depolarization of a bag cell neuron recorded on the other side, with a mean of 6.4 ± 3.4 mV (Fig. 11*A*). Moreover, bath-applying 10 mM H_2O_2, 8.3 ± 1.3 min later, evoked a burst within ~3 min, consisting of a depolarization of ~25 mV and spiking at ~0.8 Hz for ~6 min (Fig. 11*B*,*C*, black bars). In all nine clusters, administering H_2O_2 after ACh always led to spiking, as well as a significantly greater depolarization compared with the five clusters exposed to H_2O_2 alone (Fig. 11*C*).

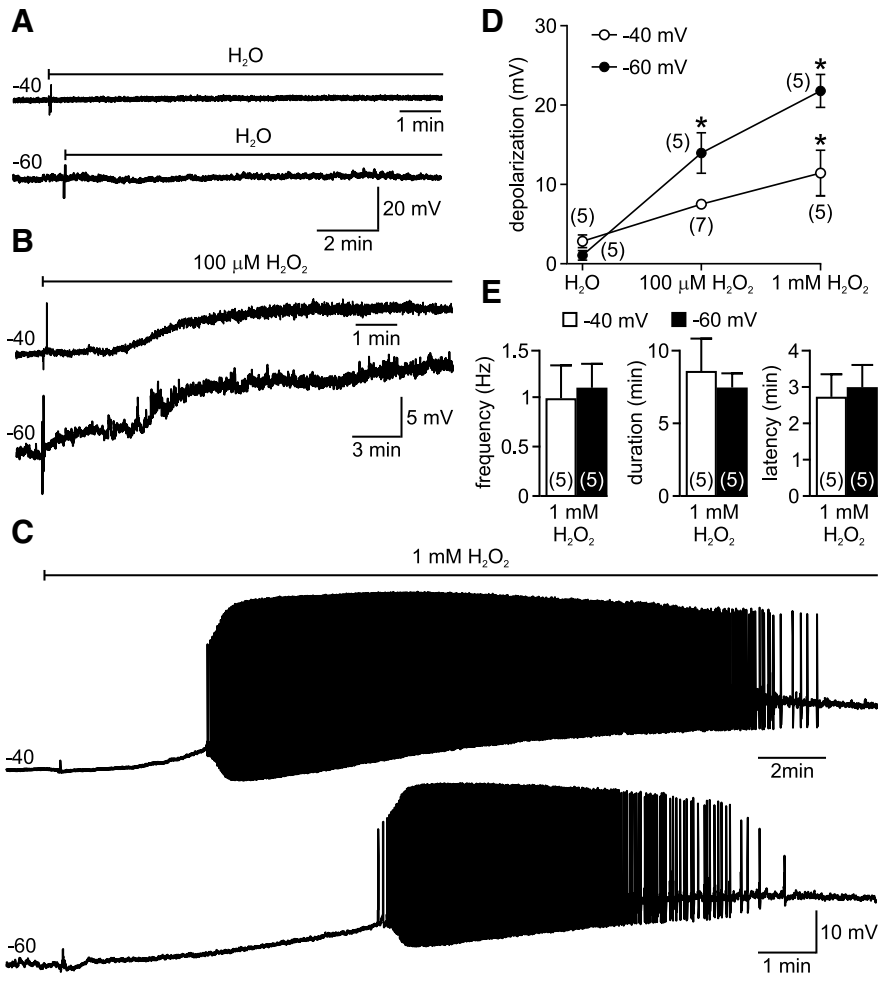

Figure 9. H_2O_2 depolarizes and induces robust action potential firing. ***A***, Separate cultured bag cell neurons are whole-cell current-clamped in nASW with K^+-based intracellular saline and initially set to either −40 or −60 mV with bias current. Bath-application (at bar) of H_2O (0.5% v/v) at −40 (top) or −60 mV (bottom) does not affect membrane voltage. Ordinate applies to both traces. ***B***, Exposure to 100 μM H_2O_2 depolarizes two different neurons from both −40 (top) and −60 (bottom) mV, but neither reaches threshold. Ordinate applies to both traces. ***C***, Delivery of 1 mM H_2O_2 depolarizes the membrane and induces robust action potential firing from both −40 (top) and −60 (bottom) mV in separate cells. Ordinate applies to both traces. ***D***, Summary graph indicating the average depolarizations from −40 (open circles) or −60 (closed circles) mV. Compared with the response produced by applying H_2O (−40 mV: 2.8 ± 0.8 mV; −60 mV: 1.1 ± 0.6 mV), the depolarization elicited by 100 μM H_2O_2 (−40 mV: 7.5 ± 0.6 mV; −60 mV: 14.0 ± 2.6 mV) or 1 mM H_2O_2 (−40 mV: 11.4 ± 2.9; −60 mV: 21.8 ± 2.1) is significantly different (−40 mV: $H = 8.545$; $df = 1$; $p = 0.0070$, KW-ANOVA; $p > 0.05$ H_2O vs 100 μM H_2O_2; $^*p < 0.05$ H_2O vs 1 mM H_2O_2, Dunn's multiple-comparison's test; −60 mV: $F_{(2,12)} = 29.275$; $p < 0.0001$, ordinary ANOVA; $^*p < 0.01$ H_2O vs 100 μM H_2O_2, $^*p < 0.001$ H_2O vs 1 mM H_2O_2, Tukey–Kramer multiple-comparisons test). ***E***, Group data show no significant difference in the frequency ($t_{(8)} = 0.2841$; $p = 0.7835$, unpaired Student's *t* test) or duration ($t_{(8)} = 0.3884$; $p = 0.7079$, unpaired Student's *t* test) of action potential firing from −40 versus −60 mV caused by 1 mM H_2O_2. In addition, there is no significant difference in the latency, i.e., the time it takes for the neuron to start firing action potentials post-H_2O_2 delivery, between responses at −40 mV (2.8 ± 0.6 mV) and −60 mV (3.0 ± 0.6 mV; $t_{(8)} = 0.3001$; $p = 0.7718$, unpaired Student's *t* test).

Discussion

H_2O_2 can oxidize DNA, lipids, or proteins (Halliwell, 1992; Gutteridge and Halliwell, 1992), which may bring about synaptic plasticity (Kamsler and Segal, 2004; Kishida and Klann, 2007) or gate ion channels (Avshalumov et al., 2007). For example, various cation currents in hippocampal, nigral, and striatal neurons are opened by H_2O_2 (Hill et al., 2006; Olah et al., 2009; Lee et al., 2013). The bag cell neuron afterdischarge is maintained by various nonselective cation channels. In the fast-phase, Ca^{2+} influx and release opens a voltage-independent cation channel, with a linear current/voltage relationship and an ~−40 mV reversal potential (Hung and Magoski, 2007; Hickey et al., 2010). With the slow-phase, phospholipase C cleaves PIP_2 into IP_3 and DAG (Fink et al., 1988). DAG gates a second, voltage-independent cation channel, with a distinct pharmacology and reversal potential of ~−20 mV (Sturgeon and Magoski, 2016). This channel may be similar to TRPC3/6/7 channels, which are well established as being activated by DAG (Hofmann et al., 1999; Okada et al., 1999). DAG also activates PKC to mediate a number of afterdischarge-associated events (DeRiemer et al., 1984; Wayne et al., 1999; Groten and Magoski, 2015), including the regulation of a third cation channel that is voltage-dependent with a reversal potential >+30 mV (Wilson et al., 1996, 1998; Magoski and Kaczmarek, 2005; Gardam and Magoski, 2009; Sturgeon and Magoski, 2018). PKC also stimulates H_2O_2 production in bag cell neurons (Munnamalai et al., 2014), suggesting that H_2O_2 may be a signaling molecule during the afterdischarge.

We find that extracellular application of H_2O_2 elicits a prolonged voltage- and concentration-dependent inward current in

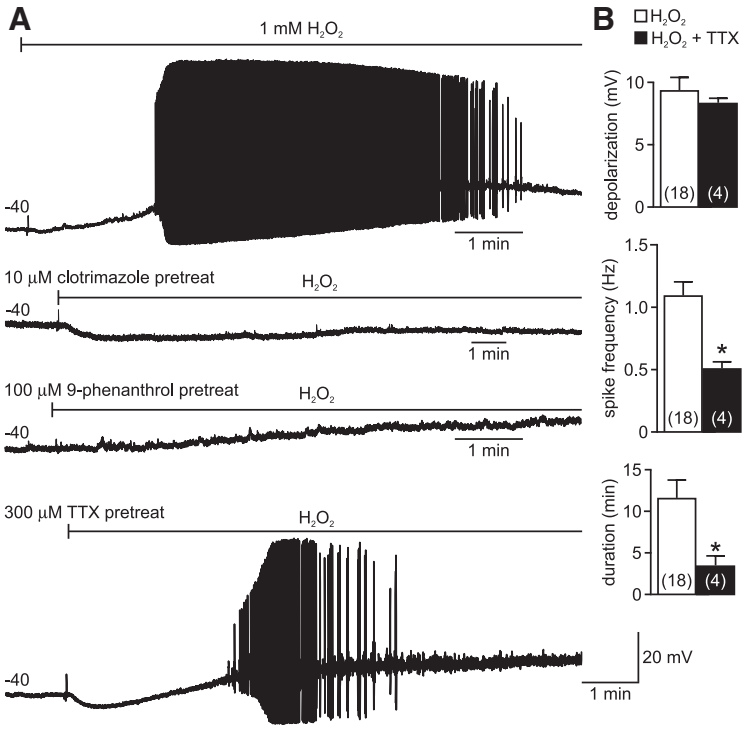

Figure 10. H_2O_2-evoked spiking is reduced by tetrodotoxin and prevented by 9-Pt or clotrimazole. Voltage responses to 1 mM H_2O_2 of different cultured bag cell neurons whole-cell current-clamped to −40 mV in nASW with K^+-based intracellular saline after 20 min pretreatment with clotrimazole, 9-Pt, or TTX. ***A***, Bath-application of 1 mM H_2O_2 (at bar) induces robust action potential firing (top). However, a 20 min pretreatment with 10 μM clotrimazole (upper middle) or 100 μM 9-phenanthrol (lower middle) virtually eliminates the depolarization and prevents firing all together. Finally, after 20 min of 300 μM TTX (bottom), introducing H_2O_2 still leads to membrane depolarization, but the duration and frequency of action potential firing is lessened. The ordinate applies to all traces. ***B***, Summary graph indicating the average H_2O_2-evoked depolarization (top) in the presence of 300 μM TTX does not differ significantly from 1 mM H_2O_2 alone ($U_{(4,18)} = 32.0$; $p = 0.7743$, Mann–Whitney *U* test). However, spike frequency (middle) and duration (bottom) are significantly reduced when TTX is in the bath (frequency: $U_{(4,18)} = 6.0$; $^*p = 0.0120$; duration: $U_{(4,18)} = 5.0$; $^*p = 0.0049$, both Mann–Whitney *U* test).

cultured bag cell neurons. The response is observed with as low as a 100 μM H_2O_2, although for consistency we primarily used 1 mM. Previous reports involving both cultured *Aplysia* sensory neurons and various mammalian neurons *in vitro* or *ex vivo* use comparable amounts of H_2O_2 and, similar to our work, show channel gating but no obvious damage (Chen et al., 2001; Chang et al., 2003; Olah et al., 2009; Lee et al., 2011, 2013; Ohashi et al., 2016). Quite possibly, these concentrations are necessary because the fast consumption of H_2O_2 by intracellular antioxidant enzymes produces a high-extracellular to low-intracellular H_2O_2 gradient, estimated by some to be up to 650-fold (Huang and Sikes, 2014). Thus, it is plausible that H_2O_2 falls substantially as it is scavenged once diffusing across the bag cell neuron membrane.

The increase in membrane conductance during the H_2O_2-induced current is consistent with channel opening, whereas the ~+30 mV reversal potential in Na^+-containing nASW suggests the conductance is nonselective for cations. Depending on specific ionic permeability, cation channels can have a wide range of reversal potentials (−40 to +50 mV; Partridge et al., 1994; Clapham, 2003). The bag cell neuron H_2O_2-induced current is dependent on select extracellular cations, i.e., the current is lessened in the absence of extracellular Ca^{2+}, diminished even further whether only Na^+ is removed, and nearly eliminated when both cations are taken away. In addition, the Ca^{2+}-, Na^+-, or Na^+/Ca^{2+}-free external salines all negatively shift the reversal potential to ~−10 mV, and drastically reduce any outward current at more positive voltages. Likely, the channel normally passes more Na^+ and Ca^{2+} into the neuron than it does K^+ out.

The U-shaped current/voltage relationship and ~+30 mV reversal potential of the H_2O_2-induced current are very similar to that of the bag cell neuron cation channel reported by Wilson et al. (1996). That channel is both sensitive to the removal of extracellular Ca^{2+}, which lowers the conductance and left-shifts the reversal potential, and is modestly blocked by intracellular Mg^{2+} (Geiger et al., 2009). For the H_2O_2-gated channel, Na^+- and/or Ca^{2+}-free saline may result in an insufficiency of extracellular cations in the pore; if those cations normally repulse intracellular Mg^{2+}, their absence could enhance the Mg^{2+} block and impede outward current. There are accounts of TRPC4/5 and TRPM2 channels passing limited outward current following replacement of extracellular Na^+ and Ca^{2+} with NMDG (Schaefer et al., 2000, 2002; Kühn and Lückhoff, 2004; Blair et al., 2009).

The pharmacology of the H_2O_2-induced current also indicates a cation channel. Both the inward current and depolarization brought about by H_2O_2 are inhibited by 9-Pt, an ostensible TRPM4-specific inhibitor (Grand et al., 2008; Guinamard et al., 2014), which also blocks the voltage-dependent cation channel (Sturgeon and Magoski, 2013), as well as clotrimazole, a general cation channel blocker that has been found to inhibit TRPM2 (Hill et al., 2004). Furthermore, pretreatment with TTX, which Wilson et al. (1996) showed blocks the voltage-dependent cation channel in bag cell neurons, prevents the H_2O_2-induced current. TTX also impacts the action potential burst elicited by H_2O_2, which is again reminiscent of Wilson et al. (1996), who found that TTX attenuates the depolarization brought about by opening the voltage-dependent cation channel. It is unlikely that TTX is effecting Na^+ channels, given that both our laboratory and others rarely observe voltage-gated Na^+ current in cultured bag cell neurons (Nick et al., 1996; Magoski et al., 2000). Based on similar biophysical and pharmacological properties, the H_2O_2-induced current and the current characterized by Wilson et al. (1996) appear to be the same or at the very least share one or more channel subunits.

Lee et al. (2011) demonstrated that inhibiting glutathione peroxidase with mercaptosuccinate increases the intracellular H_2O_2 concentration of substantia nigra neurons. Our finding that the H_2O_2-induced current is enhanced by mercaptosuccinate suggests glutathione peroxidase normally catalyzes the reduction of H_2O_2 in bag cell neurons. Fittingly, the H_2O_2-induced current is attenuated by *N*-acetylcysteine, a precursor for glutathione synthesis (Cotgreave et al., 1991). These findings are in agreement with gating by redox, where greater glutathione bioavailability lessens the current by eliminating more H_2O_2. Last, the response is decreased with dithiothreitol, which likely opposes the effects of H_2O_2 by keeping sulfhydryl groups on key Cys and/or Met residues in the reduced state (Cleland, 1964). It is presently un-

known whether redox reactions underlying activation are on associated protein(s) or directly on the channel, as is the case for inwardly rectifying K^+ channels and various TRPC or TRP vanilloid channels (Bannister et al., 1999; Yoshida et al., 2006).

TRPM2 is expressed in neurons and microglia, and can be triggered by H_2O_2 (Perraud et al., 2001; Sano et al., 2001; Kraft et al., 2004; Tong et al., 2006). An increase in endogenous H_2O_2 with mercaptosuccinate elevates the firing rate of substantia nigra GABAergic neurons by activating a TRPM2-like channel (Lee et al., 2011, 2013), possibly by oxidation of sulfhydryl groups on TRPM2 Cys residues (Ogawa et al., 2016). Our findings suggest a similar effect in bag cell neurons. NEM, an alkylating agent that is reactive toward thiols (Jakobs et al., 1982), evokes a current which appears analogous to the H_2O_2-induced current. Furthermore, addition of H_2O_2 after NEM does not induce a response and vice versa. If H_2O_2 modifies sulfhydryl groups on Cys residues, it would be unable to induce a response post-NEM application. Based on the redox-type activation mechanism we propose, the *Aplysia* current may involve a TRPM2-like subunit. That stated, the block by 9-Pt also points to a role for TRPM4-like channels, the mammalian versions of which are, like the bag cell neuron H_2O_2-induced current, voltage-dependent (Nilius et al., 2003).

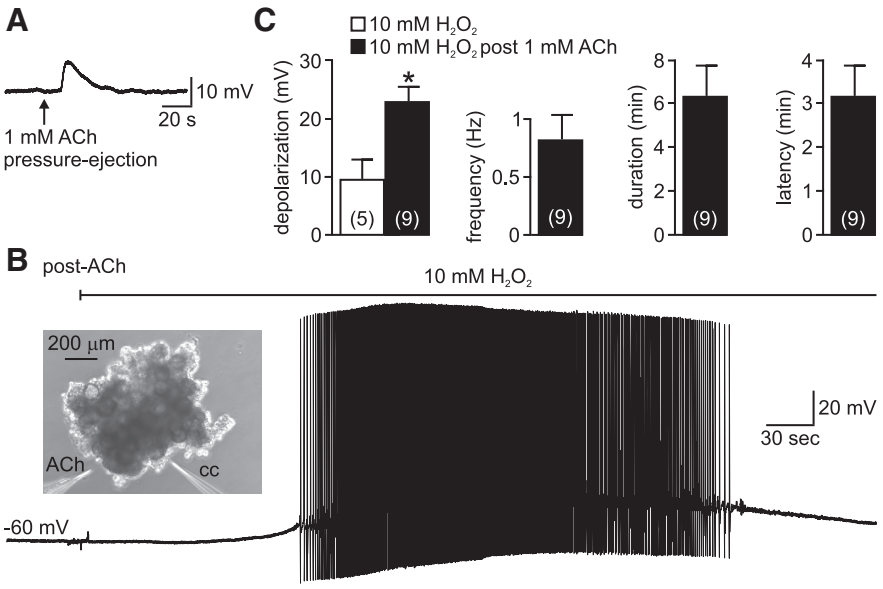

Figure 11. H_2O_2 depolarizes bag cell neurons and initiates an afterdischarge in desheathed clusters. ***A***, Under sharp-electrode current-clamp, a 2 s 1 mM ACh pressure ejection (arrow) to one side of the cluster depolarizes a bag cell neuron recorded on the opposite side. ***B***, Bath-application of 10 mM H_2O_2 (bar) post-ACh delivery initiates a prolonged burst in a bag cell neuron within a cluster. Inset, Phase-contrast photomicrograph of a desheathed bag cell neuron cluster in tcASW indicating the placement of the ACh-containing pressure ejection electrode and the intracellular current-clamp (*cc*) sharp electrode. ***C***, Following 1 mM ACh pressure ejection, 10 mM H_2O_2 is introduced 8.3 min later and induces a depolarization (23.2 ± 2.5 mV; $t_{(12)} = 3.375$; $^*p = 0.0055$, unpaired Student's *t* test) that evokes a burst, whereas 10 mM H_2O_2 alone solely depolarizes the neuron, but to a significantly lesser extent (9.8 ± 3.6 mV; left). During the H_2O_2-evoked burst, the frequency of action potential firing is 0.8 ± 0.2 Hz (left), mean discharge duration is 6.4 ± 1.4 min (middle), and the latency is 3.4 ± 0.7 min (right).

Delivery of H_2O_2 to the desheathed, isolated bag cell neuron cluster can elicit spiking. Because bath-applying H_2O_2 alone causes a burst in a minority of clusters, we speculate H_2O_2 may need to work in concert with ACh, a known input transmitter that gates an ionotropic receptor on bag cell neurons (White and Magoski, 2012; White et al., 2014). Pressure-ejecting ACh onto one side of the cluster depolarizes a neuron recorded on the opposite side; this is because of the transfer of cholinergic current through electrotonic coupling between neurons within the cluster (Kupfermann and Kandel, 1970; Dargaei et al., 2014; White et al., 2018). When H_2O_2 is bath-applied subsequent to the ACh pressure-ejection, it consistently provokes an afterdischarge-like burst. ACh may facilitate H_2O_2-dependent opening of the voltage-dependent cation channel, either through direct depolarization or initiating an as yet unidentified intracellular pathway. Work by our laboratory and others indicates that if one bag cell neuron is bursting within the cluster, all other neurons also spike synchronously (Kupfermann and Kandel, 1970; Brown and Mayeri, 1989; Dargaei et al., 2014). Thus, it is reasonable to assume that the H_2O_2-induced afterdischarge-like response represents *en masse* firing of the cluster.

Activating PKC in bag cell neurons is sufficient to turn on H_2O_2 production (Munnamalai et al., 2014). Given that PKC is triggered during the afterdischarge (Wayne et al., 1999), and H_2O_2 exposure depolarizes bag cell neurons, as well as elicits prolonged action potential firing similar to the afterdischarge, it is possible that H_2O_2 is a signaling molecule for the afterdischarge. The H_2O_2-induced nonselective cation current may maintain the afterdischarge, thereby ensuring egg-laying hormone secretion and reproductive behavior. Thus, in addition to the link between oxidative damage and various neurodegenerative diseases (Brieger et al., 2012), the production of reactive oxygen species can have a role in physiological processes.

References

Antunes LM, Darin JD, Bianchi MD (2000) Protective effects of vitamin C against cisplatin-induced nephtotoxicity and lipid peroxidation in adult rats. Pharmacol Res 41:405–411.

Arch S (1972) Polypeptide secretion from the isolated parietovisceral ganglion of *Aplysia californica*. J Gen Physiol 59:47–59.

Arch S, Smock T (1977) Egg-laying behavior in *Aplysia californica*. Behav Biol 19:45–54.

Avshalumov MV, Chen BT, Koós T, Tepper JM, Rice ME (2005) Endogenous hydrogen peroxide regulates the excitability of midbrain dopamine neurons via ATP-sensitive potassium channels. J Neurosci 25:4222–4231.

Avshalumov MV, Bao L, Patel JC, Rice ME (2007) H_2O_2 signaling in the nigrostriatal dopamine pathway via ATP-sensitive potassium channels: issues and answers. Antioxid Redox Signal 9:219–231.

Babior BM, Kipnes RS, Curnutte JT (1973) Biological defense mechanisms: the production by leukocytes of superoxide, a potential bactericidal agent. J Clin Invest 52:741–744.

Baker AL, O'Toole RJ, Gulledge AT (2018) Preferential cholinergic excitation of corticopontine neurons. J Physiol 596:1659–1679.

Bannister JP, Young BA, Main MJ, Sivaprasadarao A, Wray D (1999) The effects of oxidizing and cysteine-reactive reagents on the inward rectifier potassium channels Kir2.3 and Kir1.1. Pflugers Arch 438:868–878.

Bedard K, Krause KH (2007) The NOX family of ROS-generating NADPH oxidases: physiology and pathophysiology. Physiol Rev 87:245–313.

Blair NT, Kaczmarek JS, Clapham DE (2009) Intracellular calcium strongly potentiates agonist-activated TRPC5 channels. J Gen Physiol 133:525–546.

Brieger K, Schiavone S, Miller FJ Jr, Krause KH (2012) Reactive oxygen species: from health to disease. Swiss Med Wkly 142:w13659.

Brookes PS, Yoon Y, Robotham JL, Anders MW, Sheu SS (2004) Calcium, ATP, and ROS: a mitochondrial love-hate triangle. Am J Physiol Cell Physiol 287:C817–C833.

Brown RO, Mayeri E (1989) Positive feedback by autoexcitory neuropeptides in neuroendocrine bag cells of *Aplysia.* J Neurosci 9:1443–1451.

Chakfe Y, Bourque CW (2000) Excitatory peptides and osmotic pressure modulate mechanosensitive cation channels in concert. Nat Neurosci 3:572–579.

Chang DJ, Lim CS, Lee SH, Kaang BK (2003) Hydrogen peroxide modulates K^+ ion currents in cultured *Aplysia* sensory neurons. Brain Res 970:159–168.

Chen BT, Avshalumov MV, Rice ME (2001) H_2O_2 is a novel, endogenous modulator of synaptic dopamine release. J Neurophysiol 85:2468–2476.

Chicheportiche R, Balerna M, Lombet A, Romey G, Lazdunski M (1980) Synthesis of new, highly radioactive tetrodotoxin derivatives and their binding properties to the sodium channel. Eur J Biochem 104:617–625.

Clapham DE (2003) TRP channels as cellular sensors. Nature 426:517–524.

Cleland WW (1964) Dithiothreitol, a new protective reagent for SH groups. Biochemistry 3:480–482.

Colmers WF, Lewis DV Jr, Wilson WA (1982) Cs^+ loading reveals Na^+-dependent persistent inward current and negative slope resistance region in *Aplysia* giant neurons. J Neurophysiol 48:1191–2000.

Conn PJ, Kaczmarek LK (1989) The bag cell neurons of *Aplysia*: a model for the study of the molecular mechanisms involved in the control of prolonged animal behaviors. Mol Neurobiol 3:237–273.

Cotgreave I, Moldéus P, Schuppe I (1991) The metabolism of *N*-acetylcysteine by human endothelial cells. Biochem Pharmacol 42:13–16.

Dargaei Z, Colmers PL, Hodgson HM, Magoski NS (2014) Electrical coupling between *Aplysia* bag cell neurons: characterization and role in synchronous firing. J Neurophysiol 112:2680–2696.

DeRiemer SA, Kaczmarek LK, Lai Y, McGuinness TL, Greengard P (1984) Calcium/calmodulin-dependent protein phosphorylation in the nervous system of *Aplysia.* J Neurosci 4:1618–1625.

Derjean D, Bertrand S, Nagy F, Shefchyk SJ (2005) Plateau potentials and membrane oscillations in parasympathetic preganglionic neurones and intermediolateral neurones in the rat lumbosacral spinal cord. J Physiol 563:583–596.

Di Prisco GV, Pearlstein E, Robitaille R, Dubuc R (1997) Role of sensory-evoked NMDA plateau potentials in the initiation of locomotion. Science 278:1122–1125.

Dong HW, Hayar A, Callaway J, Yang XH, Nai Q, Ennis M (2009) Group I mGluR activation enhances Ca^{2+}-dependent nonselective cation currents and rhythmic bursting in main olfactory bulb external tufted cells. J Neurosci 29:11943–11953.

Dringen R, Kussmaul L, Hamprecht B (1998) Rapid clearance of tertiary butyl hydroperoxide by cultured astroglial cells via oxidation of glutathione. Glia 23:139–145.

Egorov AV, Hamam BN, Fransén E, Hasselmo ME, Alonso AA (2002) Graded persistent activity in entorhinal cortex neurons. Nature 420:173–178.

Fink LA, Connor JA, Kaczmarek LK (1988) Inositol trisphosphate releases intracellularly stored calcium and modulates ion channels in molluscan neurons. J Neurosci 8:2544–2555.

Fisher TE, Levy S, Kaczmarek LK (1994) Transient changes in intracellular calcium associated with a prolonged increase in excitability in neurons of *Aplysia californica.* J Neurophysiol 71:1254–1257.

Fontayne A, Dang PM, Gougerot-Pocidalo MA, El-Benna J (2002) Phosphorylation of p47phox sites by PKC alpha, beta II, delta, and zeta: effect on binding to p22phox and on NADPH oxidase activation. Biochemistry 41:7743–7750.

Gardam KE, Magoski NS (2009) Regulation of cation channel voltage and Ca^{2+} dependence by multiple modulators. J Neurophysiol 102:259–271.

Geiger JE, Hickey CM, Magoski NS (2009) Ca^{2+} entry through a nonselective cation channel in *Aplysia* bag cell neurons. Neuroscience 162:1023–1038.

Grand T, Demion M, Norez C, Mettey Y, Launay P, Becq F, Bois P, Guinamard R (2008) 9-phenanthrol inhibits human TRPM4 but not TRPM5 cationic channels. Br J Pharmacol 153:1697–1705.

Gregory JD (1955) The stability of *N*-ethylmaleimide and its reaction with sulfhydryl groups. J Am Chem Soc 77:3922–3923.

Groten CJ, Magoski NS (2015) PKC enhances the capacity for secretion by rapidly recruiting covert voltage-gated Ca^{2+} channels to the membrane. J Neurosci 35:2747–2765.

Guinamard R, Hof T, Del Negro CA (2014) The TRPM4 channel inhibitor 9-phenanthrol. Br J Pharmacol 171:1600–1613.

Gutteridge JM, Halliwell B (1992) Comments on review of free radical in biology and medicine, second edition. Free Radic Biol Med 12:93–95.

Halliwell B (1992) Reactive oxygen species and the central nervous system. J Neurochem 59:1609–1623.

Hatcher NG, Sweedler JV (2008) *Aplysia* bag cells function as a distributed neurosecretory network. J Neurophysiol 99:333–343.

Hernandes MS, Britto LR (2012) NADPH oxidase and neurodegeneration. Curr Neuropharmacol 10:321–327.

Herson PS, Ashford ML (1997) Activation of novel non-selective cation channel by alloxan and H_2O_2 in the rat insulin-secreting cell line in CRI-G1. J Physiol 501:59–66.

Herson PS, Lee K, Pinnock RD, Hughes J, Ashford ML (1999) Hydrogen peroxide induces intracellular calcium overload by activation of a non-selective cation channel in an insulin-secreting cell line. J Biol Chem 274:833–841.

Hickey CM, Geiger JE, Groten CJ, Magoski NS (2010) Mitochondrial Ca^{2+} activates a cation current in *Aplysia* bag cell neurons. J Neurophysiol 103:1543–1556.

Hickey CM, Groten CJ, Sham L, Carter CJ, Magoski NS (2013) Voltage-gated Ca^{2+} influx and mitochondrial Ca^{2+} initiate secretion from *Aplysia* neuroendocrine cells. Neuroscience 250:755–772.

Hill K, McNulty S, Randall AD (2004) Inhibition of TRPM2 channels by the antifungal agents clotrimazole and econazole. Naunyn Schmiedebergs Arch Pharmacol 370:227–237.

Hill K, Tigue NJ, Kelsell RE, Benham CD, McNulty S, Schaefer M, Randall AD (2006) Characterisation of recombinant rat TRPM2 and a TRPM2-like conductance in cultured rat striatal neurones. Neuropharmacology 50:89–97.

Hofmann T, Obukhov AG, Schaefer M, Harteneck C, Gudermann T, Schultz G (1999) Direct activation of human TRPC6 and TRPC3 channels by diacylglycerol. Nature 397:259–263.

Hoshi T, Heinemann S (2001) Regulation of cell function by methionine oxidation and reduction. J Physiol 531:1–11.

Huang BK, Sikes HD (2014) Quantifying intracellular hydrogen peroxide perturbations in terms of concentration. Redox Biol 2:955–962.

Hung AY, Magoski NS (2007) Activity-dependent initiation of a prolonged depolarization in *Aplysia* bag cell neurons: role for a cation channel. J Neurophysiol 97:2465–2479.

Jakobs KH, Lasch P, Minuth M, Aktories K, Schultz G (1982) Uncoupling of α-adrenoceptor-mediated inhibition of human platelet adenylate cyclase by *N*-ethylmaleimide. J Biol Chem 257:2829–2833.

Jones DP, Eklöw L, Thor H, Orrenius S (1981) Metabolism of hydrogen peroxide in isolated hepatocytes: relative contributions of catalase and glutathione peroxidase in decomposition of endogenously generated H_2O_2. Arch Biochem Biophys 210:505–516.

Kaczmarek LK, Jennings KR, Strumwasser F (1982) An early sodium and late calcium phase in the afterdischarge of peptide-secreting neurons of *Aplysia.* Brain Res 238:105–115.

Kamsler A, Segal M (2004) Hydrogen peroxide as a diffusible signal molecule in synaptic plasticity. Mol Neurobiol 29:167–178.

Kishida KT, Klann E (2007) Sources and targets of reactive oxygen species in synaptic plasticity and memory. Antioxid Redox Signal 9:233–244.

Knauer B, Jochems A, Valero-Aracama MJ, Yoshida M (2013) Long-lasting intrinsic persistent firing in rat CA1 pyramidal cells: a possible mechanism for active maintenance of memory. Hippocampus 23:820–831.

Knox RJ, Jonas EA, Kao LS, Smith PJ, Connor JA, Kaczmarek LK (1996) Ca^{2+} influx and activation of a cation current are coupled to intracellular Ca^{2+} release in peptidergic neurons of *Aplysia californica*. J Physiol 494:627–639.

Kourie JI (1998) Interaction of reactive oxygen species with ion transport mechanisms. Am J Physiol 275:C1–C24.

Kraft R, Grimm C, Grosse K, Hoffmann A, Sauerbruch S, Kettenmann H, Schultz G, Harteneck C (2004) Hydrogen peroxide and ADP-ribose induce TRPM2-mediated calcium influx and cation currents in microglia. Am J Physiol Cell Physiol 286:C129–C137.

Kramer RH, Zucker RS (1985) Calcium-dependent inward current in *Aplysia* bursting pace-maker neurons. J Physiol 362:107–130.

Kühn FJ, Lückhoff A (2004) A sites of the NUDT9-H domain critical for ADP-ribose activation of the cation channel TRPM2. J Biol Chem 279:46431–46437.

Kupfermann I, Kandel ER (1970) Electrophysiological properties and func-

tional interconnections of two symmetrical neurosecretory clusters (bag cells) in abdominal ganglion of *Aplysia.* J Neurophysiol 33:865–876.

Lee CR, Witkovsky P, Rice ME (2011) Regulation of substantia nigra pars reticulata GABAergic neuron activity by H_2O_2 via flufenamic acid-sensitive channels and K^+-ATP channels. Front Syst Neurosci 5:14.

Lee CR, Machold RP, Witkovsky P, Rice ME (2013) TRPM2 channels are required for NMDA-induced burst firing and contribute to H_2O_2-dependent modulation in substantia nigra pars reticulate GABAergic neurons. J Neurosci 33:1157–1568.

Lee DK, Jeong JH, Chun SK, Chua S Jr, Jo YH (2015a) Interplay between glucose and leptin signalling determines the strength of GABAergic synapses at POMC neurons. Nat Commun 6:6618.

Lee CR, Patel JC, O'Neill B, Rice ME (2015b) Inhibitory and excitatory neuromodulation by hydrogen peroxide: translating energetics to information. J Physiol 593:3431–3446.

Loechner KJ, Azhderian EM, Dreyer R, Kaczmarek LK (1990) Progressive potentiation of peptide release during a neuronal discharge. J Neurophysiol 63:738–744.

Loechner KJ, Knox RJ, Connor JA, Kaczmarek LK (1992) Hyperosmotic media inhibit voltage-dependent calcium influx and peptide release in *Aplysia* neurons. J Membr Biol 128:41–52.

Lupinsky DA, Magoski NS (2006) Ca^{2+}-dependent regulation of a non-selective cation channel from *Aplysia* bag cell neurones. J Physiol 575: 491–506.

Magoski NS, Kaczmarek LK (2005) Association/dissociation of a channel-kinase complex underlies state-dependent modulation. J Neurosci 25: 8037–8047.

Magoski NS, Knox RJ, Kaczmarek LK (2000) Activation of a Ca^{2+}-permeable cation channel produces a prolonged attenuation of intracellular Ca^{2+} release in *Aplysia* bag cell neurones. J Physiol 522:271–283.

Major G, Tank D (2004) Persistent neuronal activity: prevalence and mechanisms. Curr Opin Neurobiol 14:675–684.

Matsumoto M, Sasaki K, Sato M, Shozushima M, Takashima K (1988) Dopamine-induced depolarizing responses associated with negative slope conductance in LB-cluster neurones of *Aplysia.* J Physiol 407:199–213.

Michel S, Wayne NL (2002) Neurohormone secretion persists after post-afterdischarge membrane depolarization and cytosolic calcium elevation in peptidergic neurons in intact nervous tissue. J Neurosci 22:9063–9069.

Miller EW, Bian SX, Chang CJ (2007) A fluorescent sensor for imaging reversible redox cycles in living cells. J Am Chem Soc 129:3458–3459.

Morisset V, Nagy F (2000) Plateau potential-dependent windup of the response to primary afferent stimuli in rat dorsal horn neurons. Eur J Neurosci 12:3087–3095.

Mrejeru A, Wei A, Ramirez JM (2011) Calcium-activated non-selective cation currents are involved in generation of tonic and bursting activity in dopamine neurons of the substantia nigra pars compacta. J Physiol 589: 2497–2514.

Munnamalai V, Weaver CJ, Weisheit CE, Venkatraman P, Agim ZS, Quinn MT, Suter DM (2014) Bidirectional interactions between NOX2-type NADPH oxidase and the F-actin cytoskeleton in neuronal growth cones. J Neurochem 130:526–540.

Narahashi T, Moore JW, Scott WR (1964) Tetrodotoxin blockage of sodium conductance increase in lobster giant axons. J Gen Physiol 47:965–974.

Nick TA, Kaczmarek LK, Carew TJ (1996) Ionic currents underlying developmental regulation of repetitive firing in *Aplysia* bag cell neurons. J Neurosci 16:7583–7598.

Nilius B, Prenen J, Droogmans G, Voets T, Vennekens R, Freichel M, Wissenbach U, Flockerzi V (2003) Voltage dependence of the Ca^{2+}-activated cation channel TRPM4. J Biol Chem 278:30813–30820.

Ogawa N, Kurokawa T, Mori Y (2016) Sensing of redox status by TRP channels. Cell Calcium 60:115–122.

Ohashi M, Hirano T, Watanabe K, Katsumi K, Ohashi N, Baba H, Endo N, Kohno T (2016) Hydrogen peroxide modulates synaptic transmission in ventral horn neurons of the rat spinal cord. J Physiol 594:115–134.

Okada T, Inoue R, Yamazaki K, Maeda A, Kurosaki T, Yamakuni T, Tanaka I, Shimizu S, Ikenaka K, Imoto K, Mori Y (1999) Molecular and functional characterization of a novel mouse transient receptor potential protein homologue TRP7. Ca^{2+}-permeable cation channel that is constitutively activated and enhanced by stimulation of G protein-coupled receptor. J Biol Chem 274:27359–27370.

Olah ME, Jackson MF, Li H, Perez Y, Sun HS, Kiyonaka S, Mori Y, Tymianski M, MacDonald JF (2009) Ca^{2+}-dependent induction of TRPM2 currents in hippocampal neurons. J Physiol 587:965–979.

Partridge LD, Swandulla D (1987) Single ca-activated cation channels in bursting neurons of *Helix.* Pflugers Arch 410:627–631.

Partridge LD, Thompson SH, Smith SJ, Connor JA (1979) Current-voltage relationships of repetitively firing neurons. Brain Res 164:69–79.

Partridge LD, Müller TH, Swandulla D (1994) Calcium-activated non-selective channels in the nervous system. Brain Res Brain Res Rev 19:319–325.

Perraud AL, Fleig A, Dunn CA, Bagley LA, Launay P, Schmitz C, Stokes AJ, Zhu Q, Bessman MJ, Penner R, Kinet JP, Scharenberg AM (2001) ADP-ribose gating of the calcium-permeable LTRPC2 channel revealed by nudix motif homology. Nature 411:595–599.

Pinsker HM, Dudek FE (1977) Bag cell control of egg laying in freely behaving *Aplysia.* Science 197:490–493.

Ratté S, Karnup S, Prescott SA (2018) Nonlinear relationship between spike-dependent calcium influx and TRPC channel activation enables robust persistent spiking in neurons of the anterior cingulate cortex. J Neurosci 38:1788–1801.

Rekling JC, Feldman JL (1997) Calcium-dependent plateau potentials in rostral ambiguous neurons in the newborn mouse brain stem *in vitro.* J Neurophysiol 78:2483–2492.

Rothman BS, Weir G, Dudek FE (1983) Egg-laying hormone: direct action on the ovotestis of *Aplysia.* Gen Comp Endocrinol 52:134–141.

Roubos EW, van de Ven AM, ter Maat A (1990) Quantitative ultrastructural tannic acid study of the relationship between electrical activity and peptide secretion by the bag cell neurons of *Aplysia californica.* Neurosci Lett 111:1–6.

Sano Y, Inamura K, Miyake A, Mochizuki S, Yokoi H, Matsushime H, Furuichi K (2001) Immunocyte Ca^{2+} influx system mediated by LTRPC2. Science 293:1327–1330.

Schaefer M, Plant TD, Obukhov AG, Hofmann T, Gudermann T, Schultz G (2000) Receptor-mediated regulation of the nonselective cation channels TRPC4 and TRPC5. J Biol Chem 275:17517–17526.

Schaefer M, Plant TD, Stresow N, Albrecht N, Schultz G (2002) Functional differences between TRPC4 splice variants. J Biol Chem 277:3752–3759.

Shpak G, Zylbertal A, Yarom Y, Wagner S (2012) Calcium-activated sustained firing responses distinguish accessory from main olfactory bulb mitral cells. J Neurosci 32:6251–6262.

Sidiropoulou K, Lu FM, Fowler MA, Xiao R, Phillips C, Ozkan ED, Zhu MX, White FJ, Cooper DC (2009) Dopamine modulates an mGluR5-mediated depolarization underlying prefrontal persistent activity. Nat Neurosci 12:190–199.

Smith MA, Herson PS, Lee K, Pinnock RD, Ashford ML (2003) Hydrogen-peroxide-induced toxicity of rat striatal neurones involves activation of a non-selective cation channel. J Physiol 547:417–425.

Sohal RS, Orr WC (2012) The redox stress hypothesis of aging. Free Radic Biol Med 52:539–555.

Stuart DK, Strumwasser F (1980) Neuronal sites of action of a neurosecretory peptide, egg-laying hormone, in *Aplysia californica.* J Neurophysiol 43:499–519.

Sturgeon RM, Magoski NS (2013) Pharmacological characterization and modulation of a cation channel in *Aplysia* bag cell neurons. Soc Neurosci Abstr 39:515.16.

Sturgeon RM, Magoski NS (2016) Diacylglycerol-mediated regulation of *Aplysia* bag cell neuron excitability requires protein kinase C. J Physiol 594:5573–5592.

Sturgeon RM, Magoski NS (2018) A closely associated phospholipase C regulates cation channel function through phosphoinositide hydrolysis. J Neurosci 38:7622–7634.

Sturgeon RM, Chauhan AK, Magoski NS (2018) Neuroendocrine control of reproduction in *Aplysia* by the bag cell neurons. In: Model animals in neuroendocrinology: from worm to mouse to man (Ludwig M, Levkowitz G, eds), pp 29–58. Hoboken, NJ: Wiley.

Swandulla D, Lux HD (1985) Activation of a nonspecific cation conductance by intracellular Ca^{2+} elevation in bursting pacemaker neurons of *Helix pomatia.* J Neurophysiol 54:1430–1443.

Tahvildari B, Alonso AA, Bourque CW (2008) Ionic basis of ON and OFF persistent activity in layer III lateral entorhinal cortical principal neurons. J Neurophysiol 99:2006–2011.

Tam AK, Gardam KE, Lamb S, Kachoei BA, Magoski NS (2011) Role for

protein kinase C in controlling *Aplysia* bag cell neuron excitability. Neuroscience 179:41–55.

Tong Q, Zhang W, Conrad K, Mostoller K, Cheung JY, Peterson BZ, Miller BA (2006) Regulation of the transient receptor potential channel TRPM2 by the Ca^{2+} sensor calmodulin. J Biol Chem 281:9076–9085.

Wayne NL, Lee W, Kim YJ (1999) Persistent activation of calcium-activated and calcium independent protein kinase C in response to electrical afterdischarge from peptidergic neurons of *Aplysia.* Brain Res 834:211–213.

White SH, Magoski NS (2012) Acetylcholine-evoked afterdischarge in *Aplysia* bag cell neurons. J Neurophysiol 107:2672–2685.

White SH, Carter CJ, Magoski NS (2014) A potentially novel nicotinic receptor in *Aplysia* neuroendocrine cells. J Neurophysiol 112:446–462.

White SH, Sturgeon RM, Gu Y, Nensi A, Magoski NS (2018) Tyrosine phosphorylation determines afterdischarge initiation by regulating an ionotropic cholinergic receptor. Neuroscience 372:273–288.

Wilson GF, Richardson FC, Fisher TE, Olivera BM, Kaczmarek LK (1996) Identification and characterization of a Ca^{2+}-sensitive nonspecific cation channel underlying prolonged repetitive firing in *Aplysia* neurons. J Neurosci 16:3661–3671.

Wilson GF, Magoski NS, Kaczmarek LK (1998) Modulation of a calcium-sensitive nonspecific cation channel by closely associated protein kinase and phosphatase activities. Proc Natl Acad Sci U S A 95:10938–10943.

Yan HD, Villalobos C, Andrade R (2009) TRPC channels mediate a muscarinic receptor-induced afterdepolarization in cerebral cortex. J Neurosci 29:10038–10046.

Yoshida T, Inoue R, Morii T, Takahashi N, Yamamoto S, Hara Y, Tominaga M, Shimizu S, Sato Y, Mori Y (2006) Nitric oxide activates TRP channels by cysteine S-nitrosylation. Nat Chem Biol 2:596–607.

Zhang Y, Kaczmarek LK (2008) Bag cell neurons. Scholarpedia 3:4095.

Zhu X, Jiang M, Birnbaumer L (1998) Receptor-activated Ca^{2+} influx via human Trp3 stably expressed in human embryonic kidney (HEK) 293 cells: evidence for a non-capacitative Ca^{2+} entry. J Biol Chem 273:133–142.